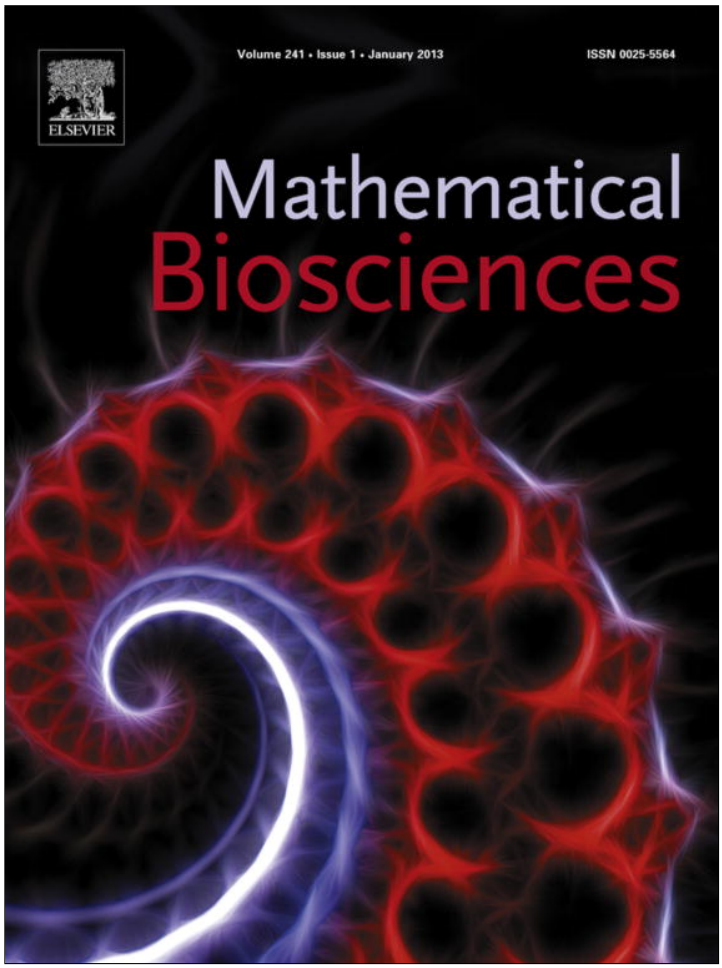

Mathematical Biosciences 241 (2013) 34–48

Contents lists available at SciVerse ScienceDirect

Mathematical Biosciences

journal homepage: www.elsevier.com/locate/mbs

Non-smooth plant disease models with economic thresholds

Tingting Zhao [a], Yanni Xiao [a], Robert J. Smith? [b,*]

[a] Department of Applied Mathematics, Xi'an Jiaotong University, Xi'an 710049, People's Republic of China
[b] Department of Mathematics and Faculty of Medicine, The University of Ottawa, 585 King Edward Ave, Ottawa, ON, Canada K1N 6N5

ARTICLE INFO

Article history:
Received 30 January 2012
Received in revised form 11 July 2012
Accepted 15 September 2012
Available online 4 October 2012

Keywords:
Plant disease
Filippov system
Lyapunov function
Integrated disease management
Economic threshold

ABSTRACT

In order to control plant diseases and eventually maintain the number of infected plants below an economic threshold, a specific management strategy called the threshold policy is proposed, resulting in Filippov systems. These are a class of piecewise smooth systems of differential equations with a discontinuous right-hand side. The aim of this work is to investigate the global dynamic behavior including sliding dynamics of one Filippov plant disease model with cultural control strategy. We examine a Lotka–Volterra Filippov plant disease model with proportional planting rate, which is globally studied in terms of five types of equilibria. For one type of equilibrium, the global structure is discussed by the iterative equations for initial numbers of plants. For the other four types of equilibria, the bounded global attractor of each type is obtained by constructing appropriate Lyapunov functions. The ideas of constructing Lyapunov functions for Filippov systems, the methods of analyzing such systems and the main results presented here provide scientific support for completing control regimens on plant diseases in integrated disease management.

1. Introduction

Plant diseases are currently one of the major threats to crops around the world, due to the fact that they carry health, social and economical problems [1,2]. The total worldwide crop loss from plant diseases is about US$220 billion dollars [3]. Therefore, it is necessary to have acceptable and effective strategies to manage epidemic development of plant diseases. It is possible to influence the course of disease development by chemical controls, which have an environmental impact because of their chemical residues. However, a wide array of measures for the control of plant diseases need to be considered, which leads to the development of integrated disease management (IDM) [4,5]. IDM combines biological, chemical and cultural tactics and so on to prevent and diminish the impact of the diseases [6]. It has been recognized that the cultural strategy of IDM — replanting of disease-free plants and roguing (i.e. identifying and removing) infected plants — is useful and effective for the control of plant diseases. For examples, the citrus tristeza virus of citrus trees, the bacterial disease in pear and apple orchards, and the fungal disease in plum are controlled by this method [7]. Hence, we examine the cultural strategy.

On the basis of IDM and the cultural strategy, in order to give a full description of the dynamics of plant disease, many different types of mathematical models on plant disease have been proposed [2,8–14]. The types most commonly used include ordinary differential equation (ODE) models, difference equation models and impulsive differential equation models. For instance, assume that the plants are divided into susceptible and infected plants and suppose the dynamics of both classes of plants is governed by the following ODE model [15]:

$$\begin{aligned} \frac{dS(t)}{dt} &= f(S(t), I(t)), \\ \frac{dI(t)}{dt} &= g(S(t), I(t)), \end{aligned} \tag{1}$$

where S, I denote the numbers of susceptible plants and infected plants, respectively; f and g represent the change rates of numbers of both classes of plants, respectively. Based on the model (1), van den Bosch et al. investigated vegetatively propagated plant diseases and made use of a mathematical model with continuous control strategies to analyze the evolution of within-plant virus titre as a response to the implementation of a range of disease-control methods [9]. In addition, a model for the temporal spread of an epidemic in a closed plant population with periodic removals of infected plants has been analyzed by Fishman et al. [14]. They compared the eradication program with no control policy and concluded that the former is economically superior.

In practice, complete eradication of the diseased plants is generally not possible, nor is it biologically or economically desirable. One of the important objectives of IDM is to minimize losses and maximize returns. IDM admits a tolerant threshold, called the economic threshold (*ET*), under which the plant damage can be acceptable. Thus, the control strategies should only be applied

* Corresponding author. Tel.: +1 613 562 5800x3864.
E-mail address: rsmith43@uottawa.ca (R.J. Smith?).

0025-5564/$ - see front matter © 2012 Elsevier Inc. All rights reserved.
http://dx.doi.org/10.1016/j.mbs.2012.09.005

when the number of diseased individuals reaches the *ET*. We term this the threshold policy. The threshold policy has shown to be easily implemented and fast-acting in IDM [16–18]. For example, Tang et al. studied a state-dependent impulsive differential equation model of plant disease with cultural control strategies and *ET* [18].

However, there exist some disadvantages in the models mentioned above. First, in the continuous models and the models with impulsive effects at fixed moments, regardless of whether the number of infected plants reaches the *ET* or not, one always exercises control. This will consume vast resources, so it is not necessary to implement control when the number of infected plants is less than the *ET*. Secondly, in the state-dependent impulsive differential models on plant diseases, the kernel of the control is that once the number of infected plants reaches *ET*, one would carry out control instantaneously and make it less than *ET* at that moment, which is not reasonable. In reality, the control strategies last some time and cannot be finished instantaneously.

Consequently, it is necessary to improve the above models to describe the reality such that non-instantaneous control is implemented in the model when the number of infected plants exceeds *ET*. Integrating the non-instantaneous control with the threshold policy, we use Filippov systems to describe the development of plant diseases [19–21]. Filippov systems have many applications in science and engineering, including harvesting thresholds, oil-well drilling and liquid–gas reactions, for which the differential equation is extended to a differential inclusion [22–27]. Although Filippov systems have been used in lots of areas, very little is known about the applications of them to the investigation of plant diseases. Consequently, our main purpose is to extend the existing models on plant diseases to be the Filippov system by considering non-instantaneous control interventions. Then, by applying the theory of Filippov systems to our proposed model, we seek conditions under which the number of infected plants can be maintained below the *ET* and susceptible plants do not go to extinction; this identifies the factors that are the most critical for controlling plant diseases. Hence, the Filippov plant disease model with proportional planting rate is formulated and analyzed. We concentrate on the following issues: Can the threshold policy guarantee the number of infected plants below the *ET* eventually? Does the limit cycle or the global attractor exist for our Filippov system? What is the difference between implementing replanting and roguing simultaneously versus carrying out only one control?

To address these questions, we initially propose a Lotka–Volterra Filippov model with proportional planting rate. Using the qualitative analysis and Lyapunov function approach, we are able to rigorously investigate the limiting set of solutions and global behavior of the system. Then the factors determining the global qualities are discussed. Finally, we make some concluding remarks on the results of this work.

2. Filippov plant disease model and preliminaries

We consider the threshold policy in plant disease modeling: once the number of infected plants exceeds the *ET*, control measures should be carried out to prevent an increasing number of infected plants from reaching the economic injury level. Whereas, if it is less than *ET*, the control measures are not necessary. A simple Filippov plant disease model based on (1) with the cultural strategy, such as replanting and roguing, can be described as follows:

$$\begin{aligned}\frac{dS(t)}{dt} &= P(S) - \beta S(t)I(t) - \eta_1 S(t) + \psi(I)pS(t),\\ \frac{dI(t)}{dt} &= \beta S(t)I(t) - \eta_2 I(t) - \psi(I)\upsilon I(t),\end{aligned} \tag{2}$$

with

$$\psi(I) = \begin{cases} 0 & \text{if} \quad I < ET,\\ 1 & \text{if} \quad I > ET,\end{cases} \tag{3}$$

where $P(S)$ is the planting number of susceptible plants per unit time; β represents the transmission rate of each infected plant, where the transmission from susceptible plants to infected plants is mediated by insects or other vectors; η_1, η_2 denote the death or harvest rates of susceptible and infected plants, respectively; p and υ represent the replanting and roguing rates, respectively. Note that here we choose the roguing proportional to the number of infected plants υI [9,18]. That is because, on the one hand, the value of the roguing rate υ could be dependent on the number of available workers; on the other hand, such a roguing term is reasonable in mathematics since the solutions can not become negative compared to constant roguing. Similarly, the replanting rate p depends on the number of available workers; moreover, such a proportional replant brings convenience in mathematical analysis. The planting function $P(S)$ could be a constant that is independent of the susceptible plants or proportional to the number of susceptible plants.

Set $H(X) = I - ET$ with $X = (S, I)^T$, and

$$\begin{aligned}F_1(X) &= (P(S) - \beta S(t)I(t) - \eta_1 S(t), \beta S(t)I(t) - \eta_2 I(t))^T,\\ F_2(X) &= (P(S) - \beta S(t)I(t) - \eta_1 S(t) + pS(t), \beta S(t)I(t)\\ &\quad - \eta_2 I(t) - \upsilon I(t))^T.\end{aligned} \tag{4}$$

We define the hyperplane

$$\Sigma = \{X \in R_+^2 | H(X) = 0\}, \tag{5}$$

which divides R_+^2 into two regions:

$$G_1 = \{X \in R_+^2 | H(X) < 0\}, \quad G_2 = \{X \in R_+^2 | H(X) > 0\}.$$

We distinguish the following regions on the discontinuity set Σ:

(i) $\Sigma_1 \subset \Sigma$ is the *sliding* region if $\langle H_X, F_1\rangle > 0$ and $\langle H_X, F_2\rangle < 0$ on Σ_1;
(ii) $\Sigma_2 \subset \Sigma$ is the *sewing* region if $\langle H_X, F_1\rangle\langle H_X, F_2\rangle > 0$ on Σ_2;
(iii) $\Sigma_3 \subset \Sigma$ is the *escaping* region if $\langle H_X, F_1\rangle < 0$ and $\langle H_X, F_2\rangle > 0$ on Σ_3,

where $\langle\cdot\rangle$ represents the scalar product and $H_X = (0, 1)^T$ is the non-vanishing gradient of H on Σ. The trajectories of (2) will stay in Σ in the sliding region Σ_1; will pass through Σ in the direction from G_1 to G_2 or from G_2 to G_1 in the sewing region; and will move either to G_1 or to G_2 in the escaping region. Note that the case (iii) does not occur in our models, since $\langle H_X, F_1\rangle < 0$ and $\langle H_X, F_2\rangle > 0$ cannot be valid simultaneously.

For the basic details and knowledge of Filippov systems, including the concepts of Filippov solution and sliding-mode solution, we refer the interested reader to the book of Filippov [19].

Solutions of (2) can be constructed by concatenating standard solutions in $G_{1,2}$ and sliding-mode solutions on Σ obtained with the well-known Filippov convex method [19] or Utkin equivalent control method [20], which are given in Appendix A. The Lambert W function [28] and various types of equilibria — such as regular, virtual and pseudo-equilibrium — play an important role in analyzing global structure of (2); the concepts of them are given in Appendix B. The notion of a Lyapunov function V, the proposition on LaSalle's Invariance Principle and its corollary for the Filippov system are given in Appendix C [29].

3. The plant disease model with proportional planting rate

A good control program would reduce the number of infected plants below a critical level, which does not induce the great losses.

Thus what we want to do next is to ensure that the number of infected plants does not exceed the ET eventually. We not only consider the threshold policy, but also take the proportional planting rate into account for the susceptible plants. The main purpose of this section is to establish the conditions that ensure achievement of our objective.

Integrating model (2) with proportional planting rate, i.e. $P(S) = \alpha S$, the Filippov plant disease model reads

$$\begin{aligned} \frac{dS(t)}{dt} &= \alpha S(t) - \beta S(t)I(t) - \eta_1 S(t) + \psi(I)pS(t), \\ \frac{dI(t)}{dt} &= \beta S(t)I(t) - \eta_2 I(t) - \psi(I)\upsilon I(t), \end{aligned} \tag{6}$$

where α represents the planting rate and $\psi(I)$ is defined in (3).

The model in G_1 becomes

$$\begin{aligned} \tfrac{dS(t)}{dt} &= \alpha S(t) - \beta S(t)I(t) - \eta_1 S(t), \\ \tfrac{dI(t)}{dt} &= \beta S(t)I(t) - \eta_2 I(t), \end{aligned} \quad I(t) > ET \tag{7}$$

and in G_2 becomes

$$\begin{aligned} \tfrac{dS(t)}{dt} &= \alpha S(t) - \beta S(t)I(t) - \eta_1 S(t) + pS(t), \\ \tfrac{dI(t)}{dt} &= \beta S(t)I(t) - \eta_2 I(t) - \upsilon I(t), \end{aligned} \quad I(t) > ET. \tag{8}$$

Here, $p > 0$ means that if $I > ET$, then we will increase the effort to grow susceptible plants when we remove the infected plants. From now on, we shall assume that $\alpha > \eta_1$. Then both (7) and (8) are Lotka–Volterra equations. It can be seen that there is a unique positive equilibrium for (7) or (8), which can be expressed as follows, respectively,

$$\begin{aligned} E_1 &= (S_1^*, I_1^*) = \left(\frac{\eta_2}{\beta}, \frac{\alpha - \eta_1}{\beta}\right) \quad \text{or} \\ E_2 &= (S_2^*, I_2^*) = \left(\frac{\eta_2 + \upsilon}{\beta}, \frac{\alpha + p - \eta_1}{\beta}\right). \end{aligned} \tag{9}$$

There exist four types of equilibria for (6): real equilibrium, virtual equilibrium, pseudoequilibrium and boundary equilibrium, which are denoted by E_R, E_V, E_P and E_B, respectively.

3.1. Sliding region and sliding-mode dynamics

A 'sliding mode' exists if there are regions in the vicinity of manifold Σ where the vectors for the two different structures of the system (6) are directed towards each other. Two basic methods were developed for a sliding mode to occur on the discontinuity surface (see details in [19,20]). It is easy to get the closure of the sliding region from its existence conditions:

$$\overline{\Sigma}_1 = \left\{(S, ET) | \frac{\eta_2}{\beta} \leqslant S \leqslant \frac{\eta_2 + \upsilon}{\beta}\right\}.$$

The sewing region is $\Sigma_2 = \{(S, ET) | S > \frac{\eta_2+\upsilon}{\beta} \text{ or } S < \frac{\eta_2}{\beta}\}$. Thus $\Sigma = \overline{\Sigma}_1 \bigcup \Sigma_2$.

Utilizing the method illustrated in Appendix A we obtain the differential equations of sliding-mode dynamics on the sliding region Σ_1,

$$\begin{aligned} \frac{dS(t)}{dt} &= \frac{\beta p}{\upsilon} S(t)^2 + \left(\alpha - \beta ET - \eta_1 - \frac{p\eta_2}{\upsilon}\right) S(t) \equiv f_1(S(t)), \\ \frac{dI(t)}{dt} &= 0, \quad (S(t), I(t)) \in \Sigma_1. \end{aligned} \tag{10}$$

Therefore, the sliding-mode dynamics are described by the first equation of (10). There exist two roots of $f_1(S(t)) = 0$ given as follows:

$$\widetilde{S}_1 = 0, \quad \widetilde{S}_2 = \frac{\beta\upsilon ET + \eta_1\upsilon + p\eta_2 - \alpha\upsilon}{\beta p}.$$

The unique pseudoequilibrium $E_P = (\widetilde{S}_2, ET)$ exists for (10) if and only if

$$\frac{\eta_2}{\beta} < \frac{\beta\upsilon ET + \eta_1\upsilon + p\eta_2 - \alpha\upsilon}{\beta p} < \frac{\eta_2 + \upsilon}{\beta}.$$

Note that the pseudoequilibrium E_P is unstable if it is feasible since $f_1'(\widetilde{S}_2) = \beta ET + \eta_1 + \frac{p\eta_2}{\upsilon} - \alpha > 0$.

3.2. Global analysis of dynamic behavior of (6)

Before showing the global behavior of the trajectories of (6), we first give the following equivalent relations.

Claim

$$\begin{aligned} &\frac{\beta\upsilon ET + \eta_1\upsilon + p\eta_2 - \alpha\upsilon}{\beta p} < \frac{\eta_2 + \upsilon}{\beta} \iff \beta ET + \eta_1 - \alpha - p < 0, \\ &\frac{\beta\upsilon ET + \eta_1\upsilon + p\eta_2 - \alpha\upsilon}{\beta p} > \frac{\eta_2}{\beta} \iff \beta ET + \eta_1 - \alpha > 0, \end{aligned}$$

which is easy to prove, so we omit it here.

It should be emphasized that, according to the coordinates of E_1 and E_2, the case that both E_1 and E_2 are virtual equilibria does not occur. For the global qualities of (6), we consider the following five cases in terms of the types of equilibrium points E_1 and E_2.

Case 3.1. Both E_1 and E_2 are real equilibria, i.e. $\frac{\alpha-\eta_1}{\beta} < ET < \frac{\alpha+p-\eta_1}{\beta}$.

In this case, E_1 and E_2 are denoted by E_R^1 and E_R^2, respectively. It follows from the Claim that there exists a unique unstable pseudoequilibrium E_P for (10). Let $(S(t), I(t))$ be any solution of system (6), the initial value of which is (S_0, I_0). Without loss of generality, we fix I_0 with $I_0 < ET$. The analysis for the case $I_0 > ET$ is similar to that for $I_0 < ET$. Set

$$\begin{aligned} &l_1 = \left\{(S, I) | S = \frac{\eta_2}{\beta}\right\}, \quad l_2 = \left\{(S, I) | S = \frac{\eta_2 + \upsilon}{\beta}\right\}, \\ &l_3 = \left\{(S, I) | I = \frac{\alpha - \eta_1}{\beta}\right\}, \quad l_4 = \left\{(S, I) | I = \frac{\alpha + p - \eta_1}{\beta}\right\}, \\ &l_5 = \{(S, I) | I = ET\}, \quad l_6 = \{(S, I) | I = I_0\}. \end{aligned} \tag{11}$$

For any given ET, there exists a closed trajectory tangent to l_5 at $D_1 = (\eta_2/\beta, ET)$ in G_1 denoted by Γ^1, and a closed trajectory tangent to l_5 at $D_3 = \left(\frac{\eta_2+\upsilon}{\beta}, ET\right)$ in G_2 denoted by Γ^2, as shown in Fig. 1. Since the pseudoequilibrium D_2 — i.e. E_P — is unstable, once the solution of (6) enters the region $|D_1D_2| = \{(S, I) | \frac{\eta_2}{\beta} < S < \widetilde{S}_2,\ I = ET\}$, then it will slide left and finally approach Γ^1. Similarly, if the solution enters the region $|D_2D_3| = \{(S, I) | \widetilde{S}_2 < S < \frac{\eta_2+\upsilon}{\beta},\ I = ET\}$, then it slides right and tends to Γ^2 eventually. It is interesting to examine where the trajectories approach if they do not enter the sliding region $|D_1D_3|$ when they intersect l_5 for the first time? Does the closed trajectory exist in $G_1 \bigcup G_2$ for system (6)?

The nonexistence of the closed trajectory in $G_1 \bigcup G_2$. Suppose there exists a closed trajectory. It follows from Fig. 1 that the only possible way for the closed trajectory in $G_1 \bigcup G_2$ is the closed curve $B_1\widehat{B_2B_1}$, where $B_1 = (S_{B_1}, ET)$ and $B_2 = (S_{B_2}, ET)$. Then, from the first integrals of (7) and (8) we have

$$\begin{aligned} &\beta(S_{B_2} - S_{B_1}) - \eta_2 \ln\left(\frac{S_{B_2}}{S_{B_1}}\right) = 0, \\ &\beta(S_{B_1} - S_{B_2}) - (\eta_2 + \upsilon) \ln\left(\frac{S_{B_1}}{S_{B_2}}\right) = 0, \end{aligned}$$

which yield

$$\beta(S_{B_1} - S_{B_2}) = (\eta_2 + \upsilon) \ln\left(\frac{S_{B_1}}{S_{B_2}}\right) = \eta_2 \ln\left(\frac{S_{B_1}}{S_{B_2}}\right).$$

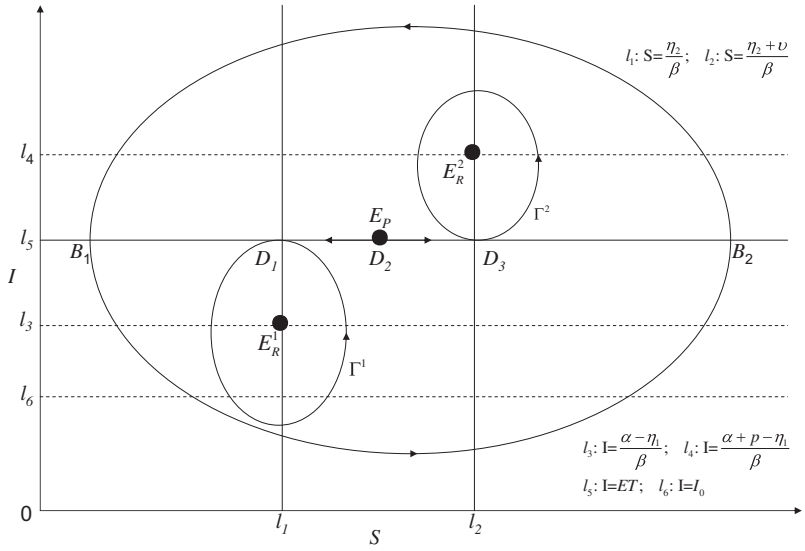

Fig. 1. Schematic diagram illustrating the nonexistence of the closed trajectory of the Filippov model (6) in Case 3.1 when E_1 and E_2 are real equilibria denoted by E_R^1 and E_R^2, respectively. D_1 and D_3 are the boundary points of the sliding region $|D_1D_3|$.

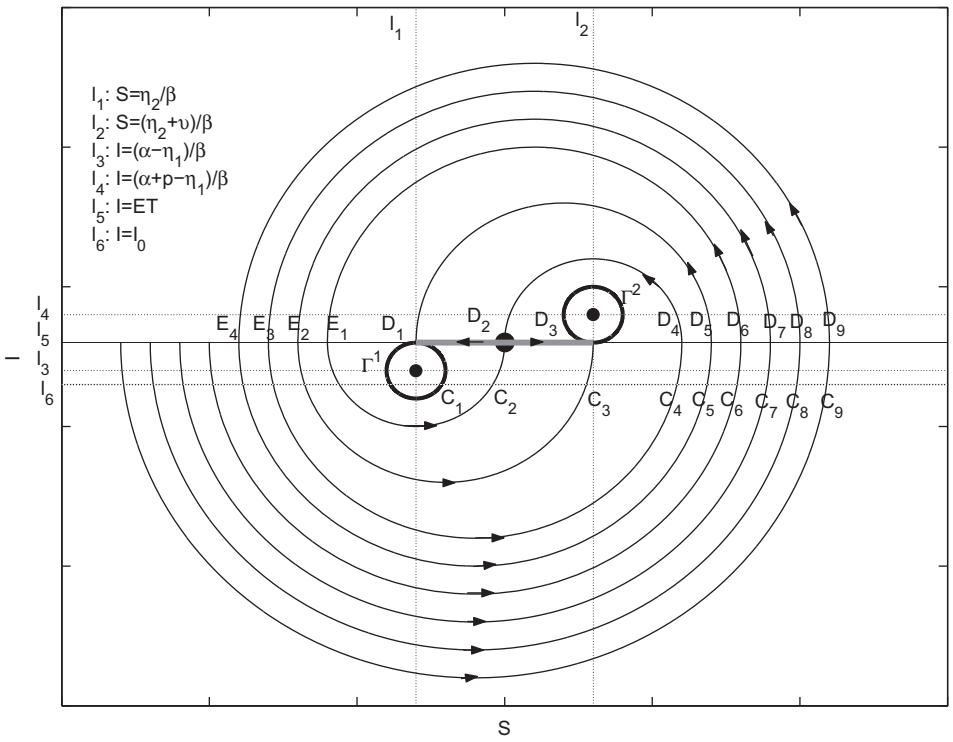

Fig. 2. Schematic diagram illustrating the basic behavior of solutions of the Filippov model (6) in Case 3.1 with different values of S_0 when E_1 and E_2 are real equilibria denoted by E_R^1 and E_R^2, respectively. D_1 and D_3 are the boundary points of the sliding region $|D_1D_3|$. Initial points of the trajectories with arrows are taken as follows: $C_2, C_3, C_4, C_5, C_6, C_7, C_8, C_9$.

This implies $\upsilon \ln\left(\frac{S_{B_1}}{S_{B_2}}\right) = 0$, which is impossible since $\upsilon \neq 0$ and $S_{B_1} \neq S_{B_2}$. Consequently, such a closed trajectory does not exist.

In order to facilitate the analysis, we use Fig. 2 to investigate the global qualities of (6). Assume that Γ^1 intersects the line l_6 at point $C_1 = (S_{C_1}, I_0)$. Since Γ^1 and Γ^2 and their interiors are the invariant sets of the Filippov system (6), and the solutions starting from the point on l_6 with $0 < S_0 < \frac{\eta_2}{\beta}$ will enter the region satisfying $S(t) > \frac{\eta_2}{\beta}$, we only consider the solution with initial values satisfying $S_0 > S_{C_1}$. All the trajectories between two adjacent trajectories described with arrows will first enter the sliding region, i.e. $|D_1D_3|$, then either approach Γ^1 or Γ^2 eventually. If the initial point belongs to the line segment $|C_1C_2|, |C_4C_5|$, $|C_5C_6|$ or $|C_8C_9|$, the corresponding trajectory will first reach $|D_1D_2|$ on l_5, and then slide left to Γ^1. Whilst, if the initial point belongs to the line segment $|C_2C_3|, |C_3C_4|, |C_6C_7|$ or $|C_7C_8|$, the corresponding trajectory will first get to $|D_2D_3|$ on l_5, and then slide right to Γ^2. Note that the trajectories of (6) consist of solutions of (7) and solutions of (8) before entering the sliding region. Suppose that a trajectory of (6) intersects with the line l_5 n_1 and n_2 times following

trajectories of (7) and (8), respectively, before entering the sliding region. Let $f_2(x)$ be the function that rounds x to the nearest integers less than or equal to x. Therefore, we denote these critical trajectories as $\Upsilon_{i,j}^m$, where m represents the ordinal of the trajectory, $i = f_2(\frac{\eta_1}{2})$ and $j = f_2(\frac{\eta_2}{2})$. Then the paths of $\Upsilon_{i,j}^m$ can be shown as follows:

(i) $\Upsilon_{0,0}^1: C_2 \to D_2$;
(ii) $\Upsilon_{0,0}^2: C_3 \to D_3$;
(iii) $\Upsilon_{0,1}^3: C_4 \to D_4 \to D_2$;
(iv) $\Upsilon_{0,1}^4: C_5 \to D_5 \to D_1$;
(v) $\Upsilon_{1,1}^5: C_6 \to D_6 \to E_1 \to \Upsilon_{0,0}^1$;
(vi) $\Upsilon_{1,1}^6: C_7 \to D_7 \to E_2 \to \Upsilon_{0,0}^2$;
(vii) $\Upsilon_{1,2}^7: C_8 \to D_8 \to E_3 \to \Upsilon_{0,1}^3$;
(viii) $\Upsilon_{1,2}^8: C_9 \to D_9 \to E_4 \to \Upsilon_{0,1}^4$,

where C_i, D_i, E_i represent the intersections of the trajectories with lines l_6, l_5 $(S(t) > \frac{\eta_2}{\beta})$ and l_5 $(S(t) < \frac{\eta_2}{\beta})$, respectively.

Using the same idea, we can also show the critical trajectories under the condition $S_0 > S_{C_9}$. It is interesting mathematically and biologically to investigate the qualities of critical trajectories, from which we can deduce the regions of the initial values of the solutions tending to Γ^1 or Γ^2. If this can be done, then we can better understand the behavior of solutions of (6). Therefore, the purpose of the following analysis is to study the initial values of the critical trajectories.

It is necessary to define the following functions:

$$\Psi_1(S(t)) = -\frac{\eta_2}{\beta}\text{Lambert W}\left(-\frac{\beta}{\eta_2}S(t)\exp\left(-\frac{\beta}{\eta_2}S(t) - Q\right)\right),$$
$$\Psi_2(S(t)) = -\frac{\eta_2+\upsilon}{\beta}\text{Lambert W}\left(-1, -\frac{\beta}{\eta_2+\upsilon}S(t)\exp\left(-\frac{\beta}{\eta_2+\upsilon}S(t)\right)\right),$$
$$\Psi_3(S(t)) = -\frac{\eta_2}{\beta}\text{Lambert W}\left(-1, -\frac{\beta}{\eta_2}S(t)\exp\left(-\frac{\beta}{\eta_2}S(t) + Q\right)\right),$$

where $Q = \frac{\beta}{\eta_2}(I_0 - ET) - \frac{\alpha-\eta_1}{\eta_2}\ln\left(\frac{I_0}{ET}\right)$. It follows from the definition of Lambert W function and the first integrals of (7) and (8) that

$$S_{C_2} = \Psi_3(\widetilde{S}_2),\ S_{C_3} = \Psi_3\left(\frac{\eta_2+\upsilon}{\beta}\right),\ S_{C_4} = \Psi_3\circ\Psi_2(\widetilde{S}_2),\ S_{C_5} = \Psi_3\circ\Psi_2\left(\frac{\eta_2}{\beta}\right),$$
$$S_{C_6} = \Psi_3\circ\Psi_2\circ\Psi_1(S_{C_2}) = \Psi_3\circ\Psi_2\circ\Psi_1\circ\Psi_3(\widetilde{S}_2),$$
$$S_{C_7} = \Psi_3\circ\Psi_2\circ\Psi_1(S_{C_3}) = \Psi_3\circ\Psi_2\circ\Psi_1\circ\Psi_3\left(\frac{\eta_2+\upsilon}{\beta}\right),$$
$$S_{C_8} = \Psi_3\circ\Psi_2\circ\Psi_1(S_{C_4}) = \Psi_3\circ\Psi_2\circ\Psi_1\circ\Psi_3\circ\Psi_2(\widetilde{S}_2),$$
$$S_{C_9} = \Psi_3\circ\Psi_2\circ\Psi_1(S_{C_5}) = \Psi_3\circ\Psi_2\circ\Psi_1\circ\Psi_3\circ\Psi_2\left(\frac{\eta_2}{\beta}\right), \tag{12}$$

where $\circ$ means the compound of functions. Then define

$$\Phi_1 = \Psi_3\circ\Psi_2\circ\Psi_1\circ\Psi_3,$$
$$\Phi_2 = \Psi_3\circ\Psi_2\circ\Psi_1\circ\Psi_3\circ\Psi_2,\quad \Phi_3 = \Psi_3\circ\Psi_2\circ\Psi_1. \tag{13}$$

Generally, the paths of the critical trajectories can be expressed as follows:

(I) $\Upsilon_{k,k}^{4(k-1)+1+4}: C_{4(k-1)+1+4+1} \to D_{4(k-1)+1+4+1} \to E_{4(k-1)+1} \to \Upsilon_{k-1,k-1}^{4(k-1)+1}$;
(II) $\Upsilon_{k,k}^{4(k-1)+2+4}: C_{4(k-1)+2+4+1} \to D_{4(k-1)+2+4+1} \to E_{4(k-1)+2} \to \Upsilon_{k-1,k-1}^{4(k-1)+2}$;
(III) $\Upsilon_{k,k+1}^{4(k-1)+3+4}: C_{4(k-1)+3+4+1} \to D_{4(k-1)+3+4+1} \to E_{4(k-1)+3} \to \Upsilon_{k-1,k}^{4(k-1)+3}$;
(IV) $\Upsilon_{k,k+1}^{4(k-1)+4+4}: C_{4(k-1)+4+4+1} \to D_{4(k-1)+4+4+1} \to E_{4(k-1)+4} \to \Upsilon_{k-1,k}^{4(k-1)+4}$,

where $S_{E_{4(k-1)+i}} = \Psi_1(S_{C_{4(k-1)+i+1}})$, $S_{D_{4(k-1)+i+4+1}} = \Psi_2(S_{E_{4(k-1)+i}})$, $S_{C_{4(k-1)+i+4+1}} = \Psi_3(S_{D_{4(k-1)+i+4+1}})$, $i = 1,2,3,4$, and $k \geqslant 1$.

Theorem 3.1. *The horizontal coordinates of the initial points of the critical trajectories can be calculated as follows:*

$$S_{C_{4k+2}} = \Phi_3^{k-1}\Phi_1(\widetilde{S}_2),\ S_{C_{4k+3}} = \Phi_3^{k-1}\Phi_1\left(\frac{\eta_2+\upsilon}{\beta}\right),$$
$$S_{C_{4k+4}} = \Phi_3^{k-1}\Phi_2(\widetilde{S}_2),\ S_{C_{4k+5}} = \Phi_3^{k-1}\Phi_2\left(\frac{\eta_2}{\beta}\right), \tag{14}$$

where Φ_3^{k-1} represents the compound of the function Φ_3 with the order $k-1, k \geqslant 1$.

We make use of induction to prove the above theorem (see Appendix D).

According to the qualitative investigation, we have the following theorem on the dynamical behavior of the solutions between the above critical trajectories.

Theorem 3.2. *If the initial value satisfies $S_0 \in \Delta$, then the solution of (6) will approach Γ^1, while if the initial value satisfies $S_0 \in (S_{C_{4k+2}}, S_{C_{4k+4}})$, then the solution of (6) will tend to Γ^2, where $\Delta = (S_{C_{4k+1}}, S_{C_{4k+2}}) \bigcup (S_{C_{4k+4}}, S_{C_{4k+5}})$ and $k \geqslant 0$.*

Thus, there exist two final trends for the solutions of the Filippov system (6). In order to better illustrate, we plot the basins of attraction of Γ^1 and Γ^2 in Fig. 3. It shows that the trajectories in the black areas will tend to Γ^1 and trajectories in the gray areas will tend to Γ^2. It is interesting to note that the black and gray areas are alternately present in the *S-I* phase plane. The object of our control is to eventually maintain the number of infected plants below the given *ET*, which will be achieved via the solutions approaching Γ^1; that is, what we need are the solutions in the black area in Fig. 3. It is thus necessary to make the initial number of the susceptible plants satisfy $S_0 \in \Delta$, since in such a situation the number of infected plants is always less than or equal to *ET* and both numbers of plants will eventually fluctuate periodically.

Case 3.2. E_1 is a real equilibrium and E_2 is a virtual equilibrium, i.e. $\frac{\alpha-\eta_1}{\beta} < \frac{\alpha+p-\eta_1}{\beta} < ET$.

For this case, E_1 and E_2 are denoted by E_R^1 and E_V^2, respectively. It indicates that $\frac{\beta\upsilon ET+\eta_1\upsilon+p\eta_2-\alpha\upsilon}{\beta p} > \frac{\eta_2+\upsilon}{\beta}$ as a result of the Claim. Hence, there is no pseudoequilibrium for (6). It follows from $S < \frac{\eta_2+\upsilon}{\beta}$ in the sliding region that

$$\frac{dS}{dt} = S\left(\frac{\beta p}{\upsilon}S + \alpha - \beta ET - \eta_1 - \frac{p\eta_2}{\upsilon}\right) < S(p + \alpha - \beta ET - \eta_1) < 0, \tag{15}$$

which implies that $S(t)$ is decreasing with respect to t in the sliding region.

Making use of the same method as Case 3.1, we could prove that in this case there is no closed trajectory similar to $\widehat{B_1B_2B_1}$ shown in Fig. 1 and we can also get the global dynamics of (6).

The solutions initiating from any point on l_6 with $S_{C_1} < S_0 \leqslant S_{C_4}$ will reach the sliding region $|AB|$, then slide left to the point A, and finally approach the closed trajectory $\widehat{C_1AC_1}$ which is tangent to the line l_5, as shown in Fig. 4.

Here, the global behavior of model (6) is obtained from the knowledge of an appropriate Lyapunov function. We set

$$V_1(S,I) = S - \frac{\eta_2}{\beta} - \frac{\eta_2}{\beta}\ln\left(\frac{S}{\frac{\eta_2}{\beta}}\right) + I - \frac{\alpha-\eta_1}{\beta} - \frac{\alpha-\eta_1}{\beta}\ln\left(\frac{I}{\frac{\alpha-\eta_1}{\beta}}\right),$$
$$V_2(S,I) = S - \frac{\eta_2+\upsilon}{\beta} - \frac{\eta_2+\upsilon}{\beta}\ln\left(\frac{S}{\frac{\eta_2+\upsilon}{\beta}}\right) + I - \frac{\alpha+p-\eta_1}{\beta} - \frac{\alpha+p-\eta_1}{\beta}\ln\left(\frac{I}{\frac{\alpha+p-\eta_1}{\beta}}\right). \tag{16}$$

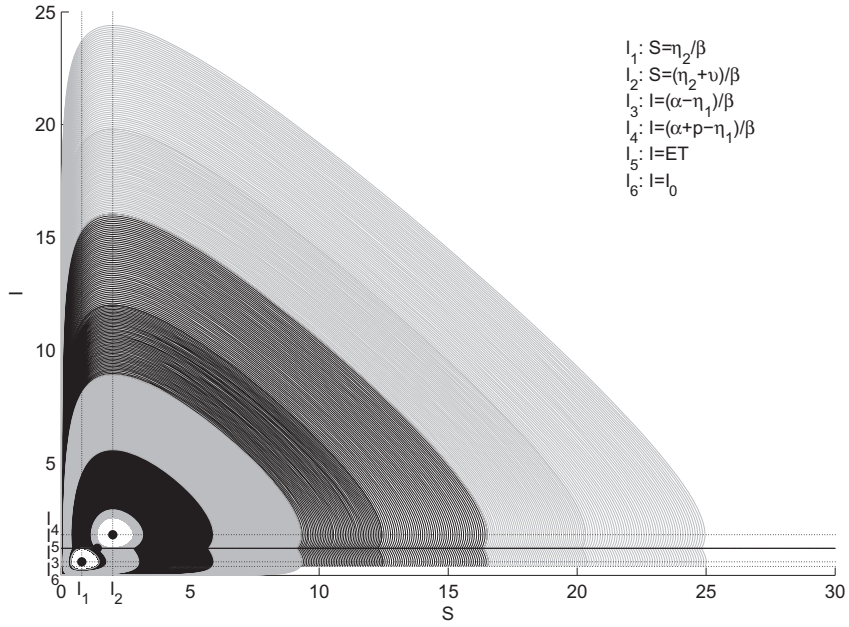

Fig. 3. Basins of attraction of Γ^{-1} and Γ^{-2} of the Filippov model (6) in Case 3.1 when E_1 and E_2 are real equilibria with $\beta = 0.5,\ \eta_1 = 0.2,\ \eta_2 = 0.4,\ p = 0.6,\ \upsilon = 0.6,\ ET = 1.2,\ \alpha = 0.5,\ I_0 = 0.4$.

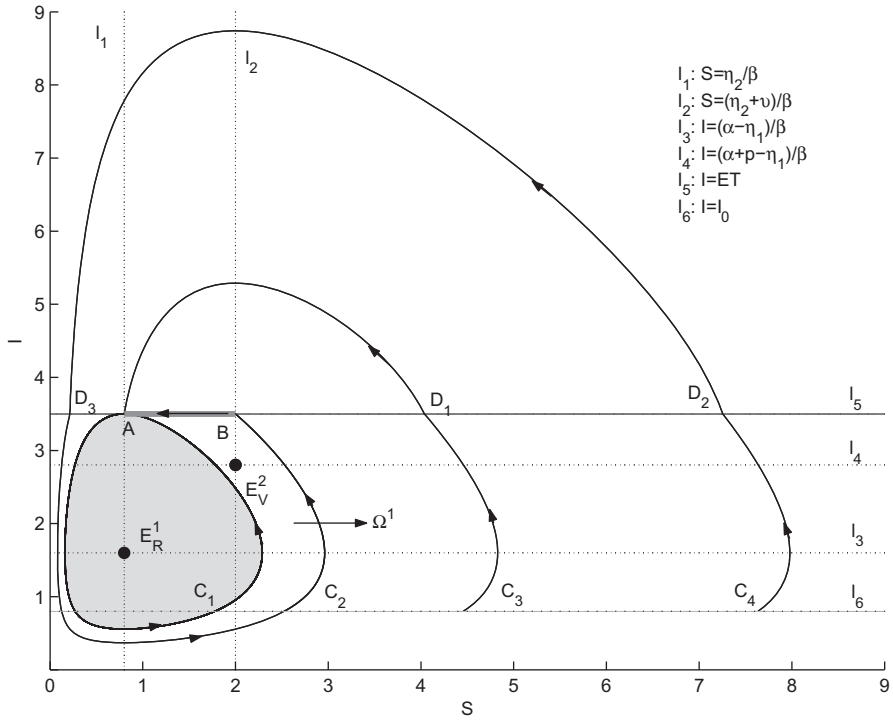

Fig. 4. Basic behavior of solutions of the Filippov model (6) in Case 3.2 with different values of S_0 when E_1 is a real equilibrium and E_2 is a virtual equilibrium denoted by E_R^1 and E_V^2, respectively. Parameters are fixed as follows: $\beta = 0.5,\ \eta_1 = 0.2,\ \eta_2 = 0.4,\ p = 0.6,\ \upsilon = 0.6,\ ET = 3.5,\ \alpha = 1,\ I_0 = 0.8$. $A = (0.8, 3.5)$ and $B = (2, 3.5)$ are the boundary points of the sliding region $|AB|$. Initial values are chosen as follows: $C_1 = (1.78, 0.8),\ C_2 = (2.53, 0.8),\ C_3 = (4.54, 0.8),\ C_4 = (7.63, 0.8)$.

Functions V_1 and V_2 are the Lyapunov functions for the differential equations (7) and (8) in the usual sense. Using these two functions, we may construct Lyapunov functions for the Filippov system (6).

Theorem 3.3. *The function* $V(S, I)$,

$$V(S,I) \equiv \begin{cases} V_1(S,I), & \text{if } I < ET, \\ V_2(S,I) + V_1(S,ET) - V_2(S,ET), & \text{if } I > ET, \\ V_2(S,I) + V_1(S,ET) - V_2(S,ET), & \text{if } I = ET,\ S \geqslant \frac{\eta_2}{\beta}, \\ V_1(S,I), & \text{if } I = ET,\ S < \frac{\eta_2}{\beta}, \end{cases} \tag{17}$$

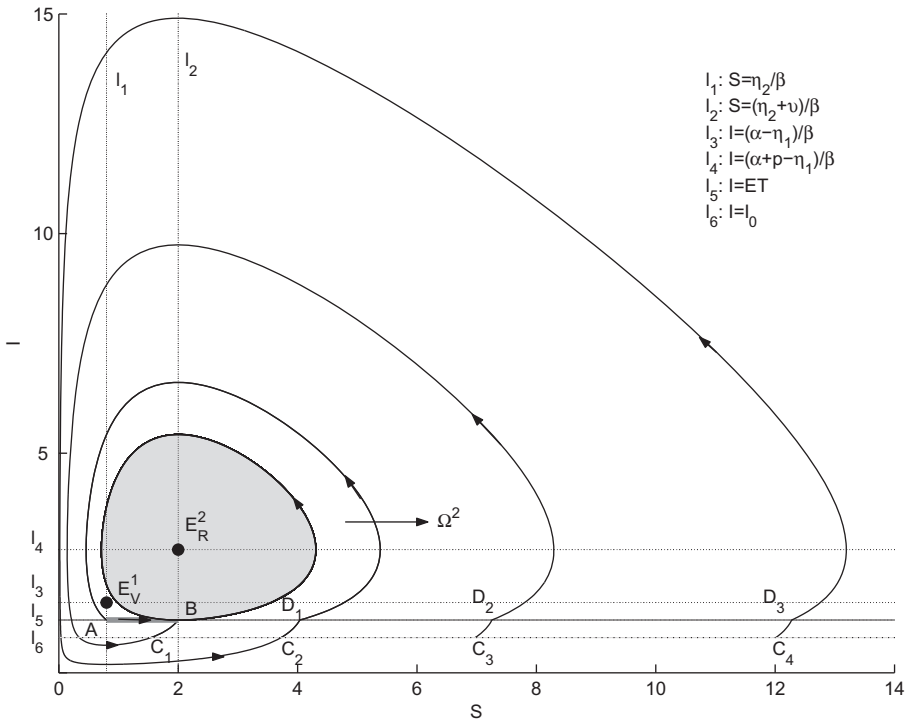

Fig. 5. Basic behavior of solutions of the Filippov model (6) in Case 3.3 with different values of S_0 when E_1 is a virtual equilibrium and E_2 is a real equilibrium denoted by E_V^1 and E_R^2, respectively. Parameters are fixed as follows: $\beta = 0.5,\ \eta_1 = 0.2,\ \eta_2 = 0.4,\ p = 0.6,\ \upsilon = 0.6,\ ET = 1.2,\ \alpha = 1,\ I_0 = 0.8$. $A = (0.8, 1.2)$ and $B = (2, 1.2)$ are the boundary points of the sliding region $|AB|$. Initial values are chosen as follows: $C_1 = (1.54, 0.8),\ C_2 = (3.72, 0.8),\ C_3 = (6.97, 0.8),\ C_4 = (12.01, 0.8)$.

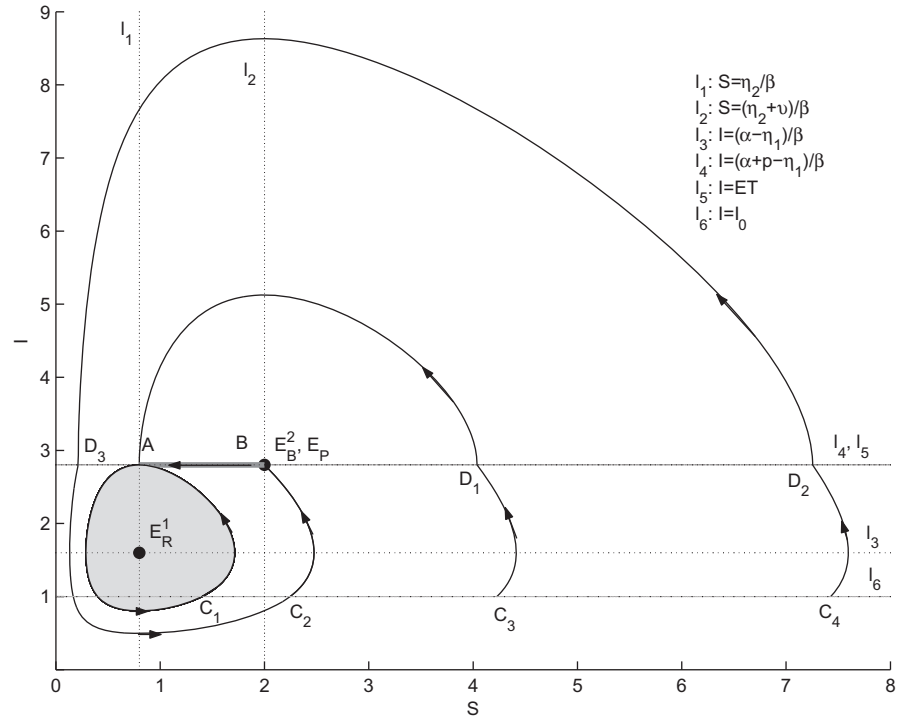

Fig. 6. Basic behavior of solutions of the Filippov model (6) in Case 3.4 with different values of S_0 when E_1 is a real equilibrium and E_2 is a boundary equilibrium denoted by E_R^1 and E_B^2, respectively. Parameters are fixed as follows: $\beta = 0.5,\ \eta_1 = 0.2,\ \eta_2 = 0.4,\ p = 0.6,\ \upsilon = 0.6,\ ET = 2.8,\ \alpha = 1,\ I_0 = 1$. $A = (0.8, 2.8)$ and $B = (2, 2.8)$ are the boundary points of the sliding region $|AB|$. Initial values are chosen as follows: $C_1 = (1.40, 1),\ C_2 = (2.25, 1),\ C_3 = (4.23, 1),\ C_4 = (7.43, 1)$.

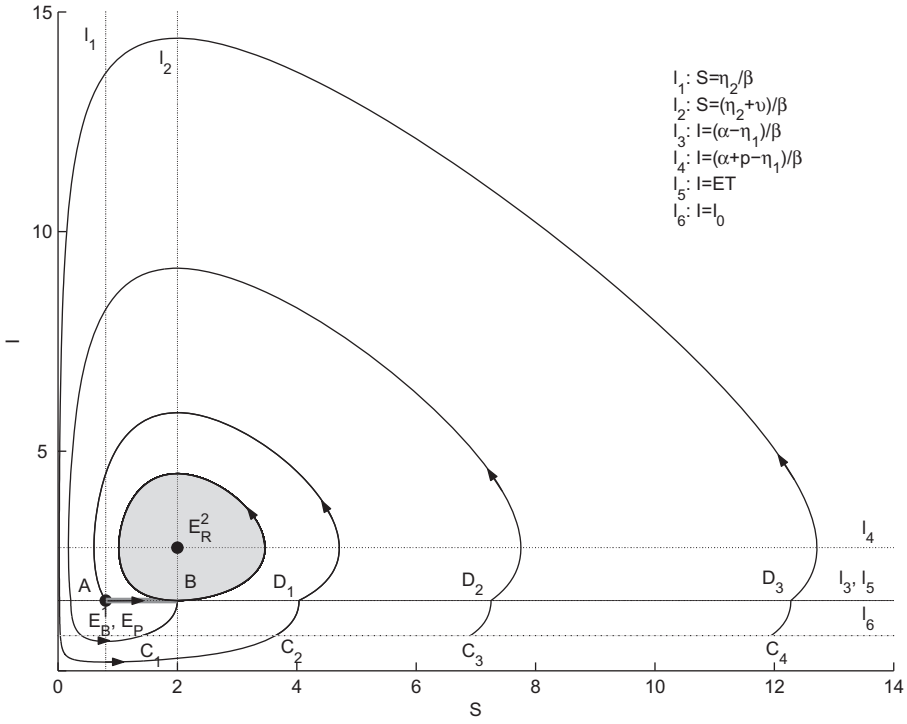

Fig. 7. Basic behavior of solutions of the Filippov model (6) in Case 3.5 with different values of S_0 when E_1 is a boundary equilibrium and E_2 is a real equilibrium denoted by E_B^1 and E_R^2, respectively. Parameters are fixed as follows: $\beta = 0.5,\ \eta_1 = 0.2,\ \eta_2 = 0.4,\ p = 0.6,\ \upsilon = 0.6,\ ET = 1.6,\ \alpha = 1,\ I_0 = 0.8$. $A = (0.8, 1.6)$ and $B = (2, 1.6)$ are the boundary points of the sliding region $|AB|$. Initial values are chosen as follows: $C_1 = (1.41, 0.8),\ C_2 = (3.65, 0.8),\ C_3 = (6.91, 0.8),\ C_4 = (11.95, 0.8)$.

Table 1
Main results of model (6) with $\alpha > 0$.

Tapes of E_1 and E_2	Conditions	Existence of pseudoequilibrium	Main results
E_R^1, E_R^2	$\frac{\alpha-\eta_1}{\beta} < ET < \frac{\alpha+p-\eta_1}{\beta}$	Yes	(I)
E_R^1, E_V^2	$\frac{\alpha-\eta_1}{\beta} < \frac{\alpha+p-\eta_1}{\beta} < ET$	No	(II)
E_V^1, E_R^2	$ET < \frac{\alpha-\eta_1}{\beta} < \frac{\alpha+p-\eta_1}{\beta}$	No	(III)
E_R^1, E_B^2	$ET = \frac{\alpha+p-\eta_1}{\beta}$	E_P and E_B^2 coincide	(II)
E_B^1, E_R^2	$ET = \frac{\alpha-\eta_1}{\beta}$	E_P and E_B^1 coincide	(III)

The superscript of E, i.e. 1 or 2, represents the equilibrium of (7) or (8), respectively. The subscript of E, i.e. R, V or B, denotes the type of equilibrium is real, virtual or boundary equilibrium, respectively. E_P is the pseudoequilibrium of (6). (I) means that if $S_0 \in \Delta$, then $I \leqslant ET$ eventually; if $S_0 \in (S_{C_{4k+2}}, S_{C_{4k+4}})$, then $I \geqslant ET$ finally; $\Gamma^1 \bigcup \Gamma^2$ and its interior is the global attractor. (II) denotes $\omega_1(R_+^2)$ is the global attractor and $I \leqslant ET$ eventually. (III) means $\omega_2(R_+^2)$ is the global attractor and $I \geqslant ET$ eventually. Here, $\Delta, \Gamma^1, \Gamma^2$ and $(S_{C_{4k+2}}, S_{C_{4k+4}}), \omega_1(R_+^2), \omega_2(R_+^2)$ are defined in Theorems 3.2, 3.3 and 3.4.

is a Lyapunov function on R_+^2 for system (6)*, and the set*

$$\omega_1(R_+^2) = \left\{(S,I) | V_1(S,I) \leqslant V_1\left(\frac{\eta_2}{\beta}, ET\right)\right\} \subset G_1 \bigcup \left(\frac{\eta_2}{\beta}, ET\right), \qquad (18)$$

is the global attractor for system (6).

Proof. If $I(t) > ET$, then it follows from $\frac{\alpha+p-\eta_1}{\beta} < ET$ that

$$\frac{\partial V_2}{\partial I} = 1 - \frac{\frac{\alpha+p-\eta_1}{\beta}}{I} > 0,$$

which yields $V_2(S, ET) < V_2(S, I)$. Hence, $V(S,I) = V_2(S,I) + V_1(S, ET) - V_2(S, ET) > 0$ provided $I(t) > ET$. It suffices to show that conditions of Proposition C.1 and Corollary C.1 introduced in Appendix C are satisfied.

By calculating, we can get the following conclusions:

(i) If $(S,I) \in G_1$, then $\langle \nabla V(S,I), F_1(S,I)\rangle = 0$.
(ii) If $(S,I) \in G_2$, then $\langle \nabla V(S,I), F_2(S,I)\rangle = \frac{\upsilon}{\beta}(\alpha - \beta I - \eta_1 + p) < \frac{\upsilon}{\beta}(\alpha - \beta ET - \eta_1 + p) < 0$.

(iii) If $(S,I) \in \Sigma$ and $S \geqslant \frac{\eta_2}{\beta}$, then

$$\langle \nabla V(S,I), F_1(S,I)\rangle = -p\left(S - \frac{\eta_2}{\beta}\right) \leqslant 0,$$

$$\begin{aligned}\langle \nabla V(S,I), F_2(S,I)\rangle &= \frac{\upsilon}{\beta}(\alpha - \beta I - \eta_1 + p)\\ &= \frac{\upsilon}{\beta}(\alpha - \beta ET - \eta_1 + p) < 0.\end{aligned}$$

Hence

$$\sup_{0\leqslant\lambda\leqslant 1} \langle \nabla V(S,I), \lambda F_1(S,I) + (1-\lambda)F_2(S,I)\rangle = 0.$$

(iv) If $(S,I) \in \Sigma$ and $S < \frac{\eta_2}{\beta}$, then

$$\langle \nabla V(S,I), F_1(S,I)\rangle = 0,$$

$$\begin{aligned}\langle \nabla V(S,I), F_2(S,I)\rangle &= pS - \upsilon I + \frac{-p\eta_2 + \alpha\upsilon - \eta_1\upsilon}{\beta}\\ &< \frac{\upsilon}{\beta}(\alpha - \eta_1 - \beta ET) < 0.\end{aligned}$$

Thus,

$$\sup_{0\leqslant\lambda\leqslant 1}\langle\nabla V(S,I),\lambda F_1(S,I)+(1-\lambda)F_2(S,I)\rangle=0.$$

It follows that $\dot{V}^*(S,I)\leqslant 0$ for all $(S,I)\in R_+^2$ and that $\Lambda=G_1\bigcup\Sigma$, where $\dot{V}^*$ and Λ are defined in Appendix C. Assume that Ω^1 consists of $\widehat{D_3C_2}B$ and the line segment $|BD_3|$, and their interiors, as shown in Fig. 4. We conclude that the largest positively invariant subset of $\overline{\Lambda}$ is Ω^1. Then, according to Proposition C.1, $\omega_1(R_+^2)$ is a subset of Ω^1. Due to the sliding mode behavior and the neutral stability of Lotka-Volterra cycles in G_1, $\omega_1(R_+^2)$ can be shown as (18), which indicates that $\omega_1(R_+^2)$ is closed. Therefore, $\omega_1(R_+^2)$ is the global attractor for system (6). □

The global attractor $\omega_1(R_+^2)$ consists of neutrally stable Lotka-Volterra trajectories. In Fig. 4, the middle gray area denotes the set $\omega_1(R_+^2)$. The trajectories cannot enter the interior of the attractor from outside. Therefore, for all initial conditions $(S_0,I_0)\notin\omega_1(R_+^2)$, we have

$$\omega_1(S_0,I_0)=\partial(\omega_1(R_+^2))=\left\{(S,I)|V_1(S,I)=V_1\left(\frac{\eta_2}{\beta},ET\right)\right\}.$$

Remark 1. The solutions with initial values outside the global attractor will first reach the sliding region and move leftwards, then approach a limit Lotka-Volterra cycle which is actually the border of the global attractor. The solutions starting from the interior of the global attractor will follow the usual Lotka-Volterra dynamics with periodic trajectories. Thus in this case, our aim, i.e. reducing the number of infected plants below a tolerable level *ET* eventually, is obtained.

Case 3.3. E_1 is a virtual equilibrium and E_2 is a real equilibrium, i.e. $ET<\frac{\alpha-\eta_1}{\beta}<\frac{\alpha+p-\eta_1}{\beta}$.

In this situation, E_1 and E_2 are denoted by E_V^1 and E_R^2, respectively. It indicates that $\frac{\beta\upsilon ET+\eta_1\upsilon+p\eta_2-\alpha\upsilon}{\beta p}<\frac{\eta_2}{\beta}$. Hence, there is no pseudoequilibrium for (6). It follows from $S>\frac{\eta_2}{\beta}$ in the sliding region that

$$\frac{dS}{dt}=S\left(\frac{\beta p}{\upsilon}S+\alpha-\beta ET-\eta_1-\frac{p\eta_2}{\upsilon}\right)>S(\alpha-\beta ET-\eta_1)>0, \tag{19}$$

which yields that $S(t)$ is increasing with respect to t in the sliding region.

For this case, the behavior of system (6) bears some analogy with the one in 3.2.

The solutions will first reach the line segment $|AB|$, then slide right to the point B and approach the closed trajectory tangent to the line l_5, i.e. the boundary of the middle gray area, as shown in Fig. 5. System (6) can also be globally studied via a Lyapunov function.

Theorem 3.4. *The function* $V(S,I)$,

$$V(S,I)\equiv\begin{cases}V_2(S,I), & \text{if } I>ET,\\ V_1(S,I)+V_2(S,ET)-V_1(S,ET), & \text{if } I<ET,\\ V_1(S,I)+V_2(S,ET)-V_1(S,ET), & \text{if } I=ET,\ S\leqslant\frac{\eta_2+\upsilon}{\beta},\\ V_2(S,I), & \text{if } I=ET,\ S>\frac{\eta_2+\upsilon}{\beta},\end{cases} \tag{20}$$

is a Lyapunov function on R_+^2 *for system* (6), *and the set*

$$\omega_2(R_+^2)=\left\{(S,I)|V_2(S,I)\leqslant V_2\left(\frac{\eta_2+\upsilon}{\beta},ET\right)\right\}\subset G_2\bigcup\left(\frac{\eta_2+\upsilon}{\beta},ET\right), \tag{21}$$

is the global attractor for system (6).

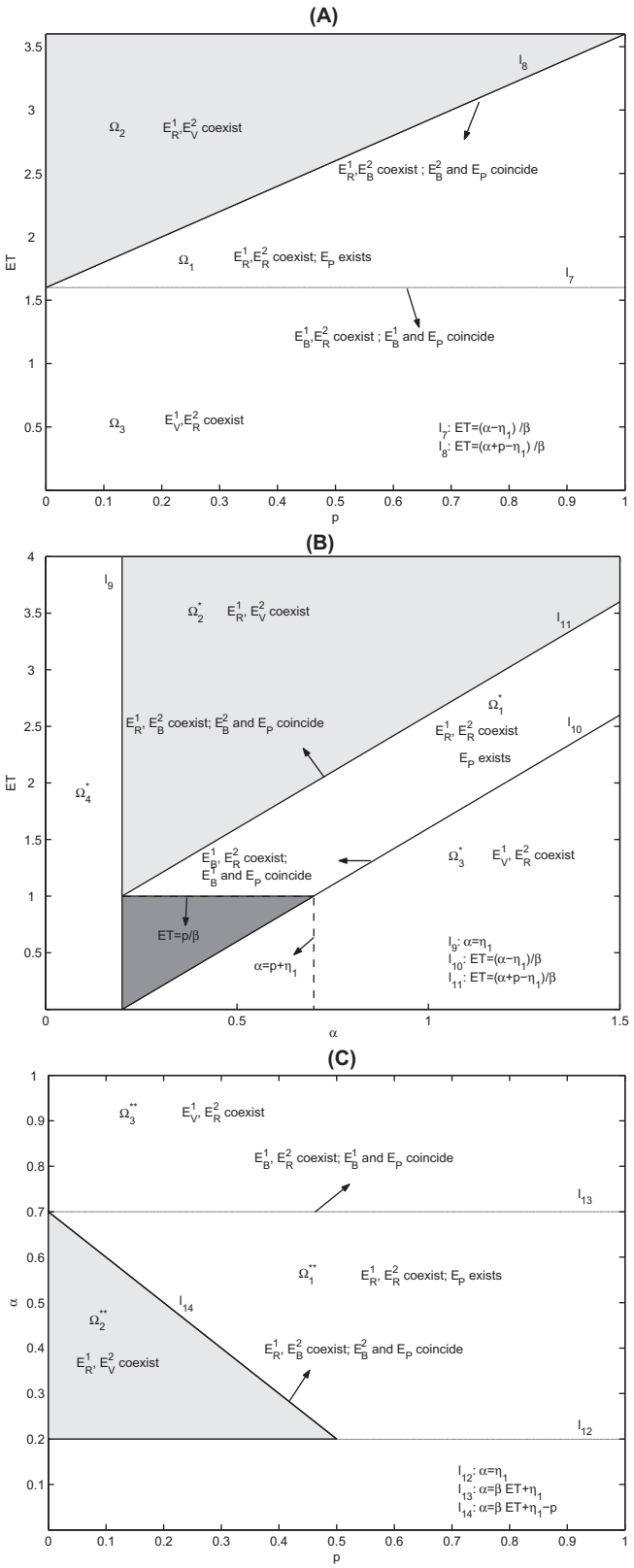

Fig. 8. Bifurcation set for Filippov system (6) with respect to (A) p and ET; (B) α and ET; (C) p and α. Here we fix all other parameters as follows: (A) $\beta=0.5,\ \eta_1=0.2,\ \alpha=1.$ (B) $\beta=0.5,\ \eta_1=0.2,\ p=0.5.$ (C) $\beta=0.5,\ \eta_1=0.2,\ ET=1.$

We can use the same method as Theorem 3.3 to prove Theorem 3.4, so we omit that here. It follows from Theorem 3.4 that $\Lambda=G_2\bigcup\Sigma$. Suppose that the Ω^2 consists of $\widehat{D_1A}$ and the line

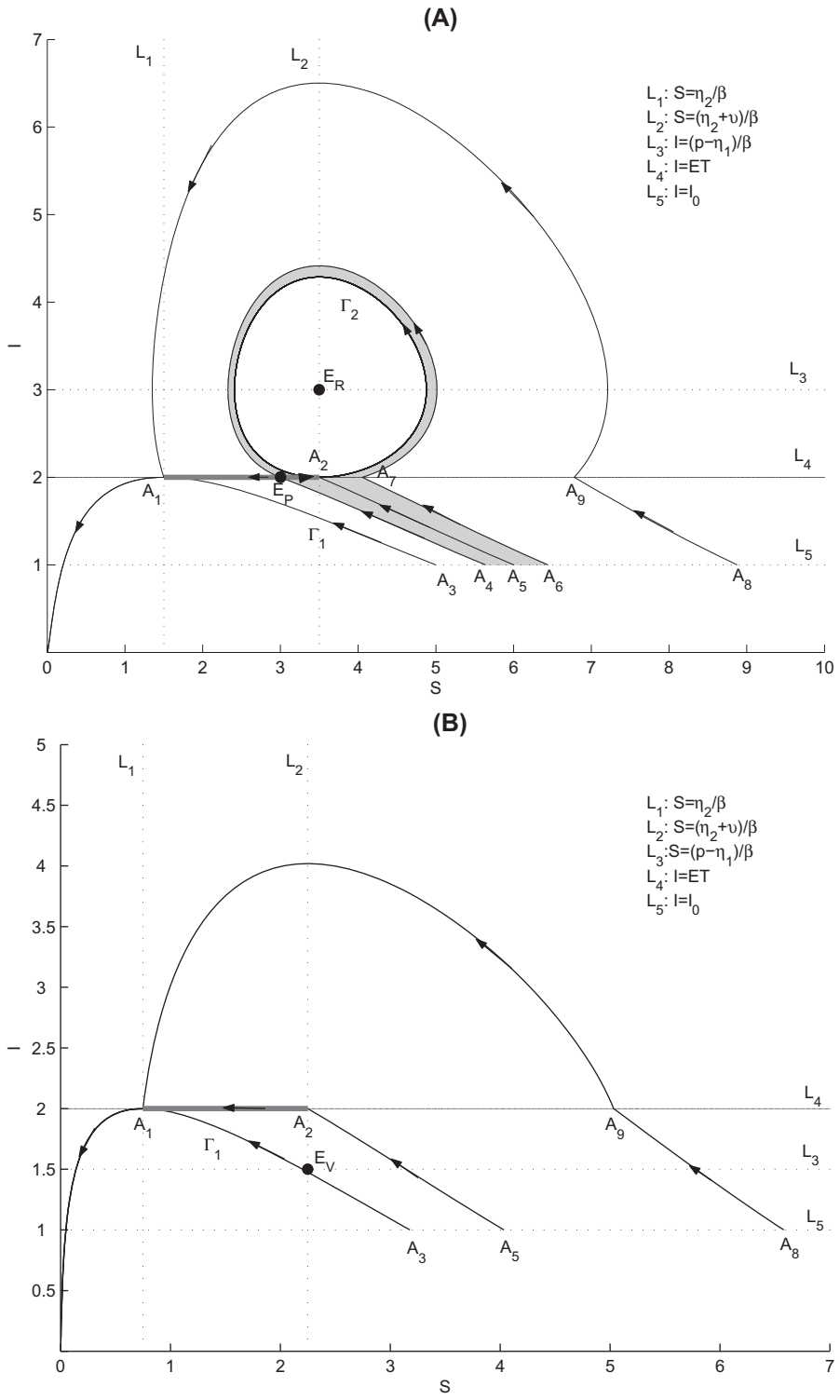

Fig. 9. Basic behavior of solutions of the Filippov model (6) with $\alpha = 0$ with different values of S_0. (A) E_2 is a real equilibrium denoted by E_R. Parameters are fixed as follows: $\beta = 0.2,\ \eta_1 = 0.2,\ \eta_2 = 0.3,\ p = 0.8,\ \upsilon = 0.4,\ ET = 2,\ I_0 = 1$. $A_1 = (1.5, 2)$ and $A_2 = (3.5, 2)$ are the boundary points of the sliding region $|A_1A_2|$. Initial values are chosen as follows: $A_3 = (5.00, 1),\ A_4 = (5.64, 1),\ A_5 = (6.00, 1),\ A_6 = (6.44, 1),\ A_8 = (8.88, 1)$. (B) E_2 is a virtual equilibrium denoted by E_V. Parameters are fixed as follows: $\beta = 0.4,\ \eta_1 = 0.2,\ \eta_2 = 0.3,\ p = 0.8,\ \upsilon = 0.6,\ ET = 2,\ I_0 = 1$. $A_1 = (0.75, 2)$ and $A_2 = (2.25, 2)$ are the boundary points of the sliding region $|A_1A_2|$. Initial values are chosen as follows: $A_3 = (3.18, 1),\ A_5 = (4.35, 1),\ A_8 = (6.58, 1)$.

segment $|AD_1|$ and their interiors in Fig. 5. Then the largest positively invariant subset of $\overline{\Lambda}$ is Ω^2. According to Proposition C.1, $\omega_2(R_+^2)$ is a subset of Ω^2 and can be written as (21), which demonstrates that $\omega_2(R_+^2)$ is closed. In Fig. 5, the middle gray area denotes the set $\omega_2(R_+^2)$. For the initial point satisfying $(S_0, I_0) \notin \omega_2(R_+^2)$, it is easy to see that

$$\omega_2(S_0,I_0)=\partial(\omega_2(R_+^2))=\left\{(S,I)|V_2(S,I)=V_2\left(\frac{\eta_2+\upsilon}{\beta},ET\right)\right\}.$$

Remark 2. Any trajectory initiating from the outside of the set $\omega_2(R_+^2)$ will approach the $\partial(\omega_2(R_+^2))$ eventually. Any trajectory starting from the interior of $\omega_2(R_+^2)$ will follow the dynamics of system (8) and hence exhibit periodic oscillation. Note that, in this case, the eventual number of infected plants is larger than or equal to the *ET*, which is not our desire, since this will cause great economic losses. Therefore, in practice, we would like to avoid this situation.

Case 3.4. E_1 is a real equilibrium and E_2 is a boundary equilibrium, i.e. $ET=\frac{\alpha+p-\eta_1}{\beta}$.

For this situation, we denote E_1 as E_R^1 and E_2 as E_B^2. It is easy to see that $\widetilde{S}_2=\frac{\eta_2+\upsilon}{\beta}$. Thus, E_P and E_B^2 coincide at the point $B=\left(\frac{\eta_2+\upsilon}{\beta},ET\right)$ and l_4 coincides with l_5, as shown in Fig. 6. Comparing Fig. 6 and Fig. 4, we see that the dynamics of Filippov system (6) in 3.4 is similar to 3.2. Therefore, there exists a global attractor $\omega_1(R_+^2)$ given by (18), which consists of $C_1\widehat{AC}_1$ and its interior. The middle gray area in Fig. 6 denotes the $\omega_1(R_+^2)$.

Case 3.5. E_1 is a boundary equilibrium and E_2 is a real equilibrium, i.e. $ET=\frac{\alpha-\eta_1}{\beta}$.

In this case, we denote E_1 as E_B^1 and E_2 as E_R^2. It is easy to yield $\widetilde{S}_2=\frac{\eta_2}{\beta}$. E_P and E_B^1 coincide at the point $A=\left(\frac{\eta_2}{\beta},ET\right)$ and l_3 coincides with l_5, as shown in Fig. 7. It follows from Fig. 7 and Fig. 5 that the solutions of Filippov system (6) in 3.5 and 3.3 have the analogous dynamical behavior. Therefore, the global attractor $\omega_2(R_+^2)$ exists and can be expressed by (21), which consists of the trajectory going through the point B and tangent to the line l_5 and its interior. In Fig. 7, the middle gray area denotes the set $\omega_2(R_+^2)$.

So far, the global dynamics of the Filippov plant disease system (6) have been investigated and the main results obtained above are summarized in Table 1. For the result (I), our control object — that is, ensuring the number of infected plants does not exceed the *ET* eventually — can be reached under some conditions for the initial values. For the result (II), our goal can be achieved, while for the result (III) our target fails to be reached.

3.3. The effects of parameters on dynamics of system (6)

It follows from the above global analysis that α and p are two factors in determining the dynamics of the system (6). To address the richness of the possible equilibria of (6), we let parameters p and *ET* vary and fix other parameters to build the bifurcation diagram, as shown in Fig. 8A. Define

$$l_7=\left\{(p,ET)|ET=\frac{\alpha-\eta_1}{\beta}\right\},\quad l_8=\left\{(p,ET)|ET=\frac{\alpha+p-\eta_1}{\beta}\right\}.$$

The lines l_7 and l_8 divide the *p*-*ET* parameter space into three regions, Ω_1,Ω_2 and Ω_3, and the existence of various types of equilibria is indicated in each region. The ranges of parameters in Cases 3.1, 3.2, 3.3, 3.4 and 3.5 correspond to $\Omega_1,\Omega_2,\Omega_3$, l_8 and l_7, respectively. As a result of the previous discussion, it is clear that the gray area of Fig. 8A, which consists of Ω_2 and l_8, is the region in which our goal of controlling plant diseases can always be achieved. If parameters are selected from Ω_1, the goal may be reached depending on the initial numbers of both plants. The number of infected plants is always more than the given *ET* if the parameters are set in Ω_3 or l_7; however, this is not what we pursue. All in all, if other parameters are fixed and the given *ET* is relatively small, i.e. less than or equal to $\frac{\alpha-\eta_1}{\beta}$, then no matter what the value of p is, we cannot reach the target since the number of infected plants is greater than the *ET* eventually. If the *ET* is relatively large, i.e. greater than $\frac{\alpha-\eta_1}{\beta}$, then our objective can always be achieved provided $0<p\leqslant\beta ET+\eta_1-\alpha$, and may be reached in some cases provided $p>\beta ET+\eta_1-\alpha$, depending on the initial conditions. Therefore, if we adjust the replanting rate for the susceptible plants p to control the plant diseases, then the number of infected plants will not be less than the threshold finally unless the threshold *ET* is relatively large.

Next, we let parameters α and *ET* change and fix other parameters to build the bifurcation diagram, as shown in Fig. 8B. Define

$$l_9=\{(\alpha,ET)|\alpha=\eta_1\},\quad l_{10}=\left\{(\alpha,ET)|ET=\frac{\alpha-\eta_1}{\beta}\right\},$$
$$l_{11}=\left\{(\alpha,ET)|ET=\frac{\alpha+p-\eta_1}{\beta}\right\}.$$

Here, suppose $p>\eta_1$. The lines l_9,l_{10} and l_{11} divide the α-*ET* parameter space into four regions, Ω_i^*, with $i=1,2,3,4$. Since $\alpha<\eta_1$ in Ω_4^*, our above discussions focus on $R_+^2\setminus\Omega_4^*$. The ranges of parameters in Cases 3.1, 3.2, 3.3, 3.4 and 3.5 correspond to Ω_1^*, $\Omega_2^*,\Omega_3^*,l_{11}$ and l_{10}, respectively. The middle gray area consists of Ω_2^* and l_{11}, in which our aim is always achieved. For a smaller threshold, i.e. *ET* less than or equal to p/β, we can choose the parameters in the dark gray area in Ω_1^*, so that the goal may be reached, depending on the initial values of both plants. For a larger threshold, i.e. *ET* greater than p/β, the parameters can be chosen in Ω_1^* with appropriate initial conditions or in the middle gray area so that the number of infected plants can be maintained below *ET* eventually. For the case of $p\leqslant\eta_1$, we will get similar conclusions.

From the above analysis, it is natural to ask how the parameters p and α jointly affect the dynamic behavior of system (6) if *ET* is fixed. We use Fig. 8C to address this. Define

$$l_{12}=\{(p,\alpha)|\alpha=\eta_1\},l_{13}=\{(p,\alpha)|\alpha=\beta ET+\eta_1\},l_{14}$$
$$=\{(p,\alpha)|\alpha=\beta ET+\eta_1-p\}.$$

The above three lines divide the parameter space into four parts. Because $\alpha>\eta_1$ holds in our discussions, we consider the issue in Ω_i^{**}, $i=1,2,3,l_{13}$ and l_{14}. The conditions $\alpha<\beta ET+\eta_1$ and $\alpha+p>\beta ET+\eta_1$, corresponding to Case 3.1, are valid in Ω_1^{**}. The ranges of $\alpha\geqslant\beta ET+\eta_1$, $\alpha+p>\beta ET+\eta_1$, corresponding to Cases 3.3 and 3.5, are satisfied in Ω_3^{**} and l_{13}; the ranges of $\alpha<\beta ET+\eta_1$ and $\alpha+p\leqslant\beta ET+\eta_1$, corresponding to Cases 3.2 and 3.4, hold true in Ω_2^{**} and l_{14}. From these correspondences, we conclude the following results. First, suppose the planting rate α is relatively small, i.e. less than $\beta ET+\eta_1$. If the replanting rate p is so small that the parameters belong to the gray area — that is, the condition $\alpha+p\leqslant\beta ET+\eta_1$ holds — then the number of infected plants can always be eventually reduced below the threshold. If p is relatively large so that $\alpha+p>\beta ET+\eta_1$, i.e. $(\alpha,p)\in\Omega_1^{**}$, then the objective is achieved by choosing the initial number of plants to satisfy the condition that $S_0\in\Delta$, where $\Delta=(S_{C_{4k+1}},S_{C_{4k+2}})\bigcup(S_{C_{4k+4}},S_{C_{4k+5}}),k\geqslant 0$, as shown in (14). Secondly, assume α is relatively large, i.e. greater

Table 2
Main results of model (6) with $\alpha=0$.

Tapes of E_2	Conditions	Existence of pseudoequilibrium	Main results
E_R	$ET<\frac{p-\eta_1}{\beta}$	Yes	(i)
E_V	$ET>\frac{p-\eta_1}{\beta}$	No	(ii)
E_B	$ET=\frac{p-\eta_1}{\beta}$	E_P and E_B coincide	(ii)

The subscript of E, i.e. R, V or B, denotes the type of E_2 is real, virtual or boundary equilibrium, respectively. E_P is the pseudoequilibrium of (6). (i) means that both plants either tend to Γ_2 or go to the origin eventually, depending on initial values. (ii) denotes both plants approach extinction.

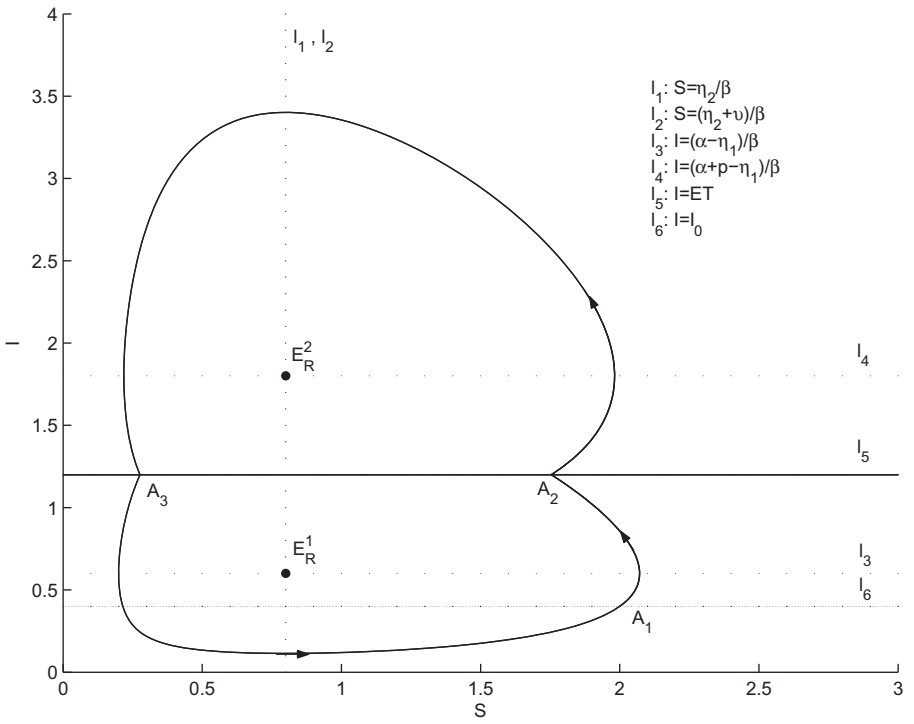

Fig. 10. Basic behavior of the solution of the Filippov model (6) with $\upsilon = 0$ when E_1 and E_2 are real equilibria denoted by E_R^1 and E_R^2, respectively. Parameters are fixed as follows: $\beta = 0.5, \eta_1 = 0.2, \eta_2 = 0.4, p = 0.6, ET = 1.2, \alpha = 0.5$. Initial value is taken as follows $A_1 = (S_0, I_0) = (2, 0.4)$.

than or equal to $\beta ET + \eta_1$. Then, no matter what the value of p is, the number of infected plants will eventually exceed the threshold, so our target fails to be achieved. Therefore, the dynamic behavior of (6) can be determined by the planting and replanting rates. The above information can guide our production practices.

Remark 3. By using similar analysis as Subsection , we could get the main results for the special system (6) with null-planting rate ($\alpha = 0$). Note that the null-planting rate has been considered by Tang et al. in the model with *ET* [18].

Case 3.1 corresponds to the situation where E_2 is a real equilibrium denoted by E_R, i.e. $ET < \frac{p-\eta_1}{\beta}$. The stable origin with $\alpha = 0$ corresponds to E_1 with $\alpha > 0$, for the model (7). For any given *ET*, there is a phase trajectory of model (7) denoted by Γ_1, starting from the point A_3 on L_5 ($L_5 : I = I_0$), tangent to the line L_4 ($L_4 : I = ET$), at the point $A_1 = (\eta_2/\beta, ET)$. There also exists a closed trajectory of the model (8), denoted by Γ_2, that is tangent to L_4 at $A_2 = (\frac{\eta_2+\upsilon}{\beta}, ET)$, as shown in Fig. 9A. The trajectory starting from a point on L_5 with $S_{A_3} < S_0 < S_{A_8}$ will enter the sliding region $|A_1A_2|$ with the pseudo-equilibrium E_P. However, only the solutions in the middle gray area, which start from the segment $|A_4A_6|$, approach the closed trajectory Γ_2 eventually; others will eventually approach $(0, 0)$.

Case 3.2 corresponds to the situation where E_2 is a virtual equilibrium denoted by E_V, i.e. $ET > \frac{p-\eta_1}{\beta}$. The trajectories with initial values satisfying $S_{A_3} < S_0 < S_{A_8}$ will experience sliding motion. All solutions starting from any point on the line L_5 will tend to the origin, which reveals that both susceptible and infected plants with arbitrary initial numbers always go to extinction, as shown in Fig. 9B.

Case 3.4 corresponds to the situation where E_2 is a boundary equilibrium denoted by E_B, i.e. $ET = \frac{p-\eta_1}{\beta}$. We note that the dynamics of (6) in this case are similar to the above situation. Therefore, all the solutions starting from any point on the line L_5 will eventually tend to zero. In addition, Cases 3.3 and 3.5 do not exist under the condition $\alpha = 0$.

The main results obtained here are displayed in Table 2, which demonstrates that the numbers of susceptible and infected plants either go to zero or oscillate periodically with $I \geqslant ET$. Therefore, in this scenario of null-planting rate, we fail to control plant diseases.

4. Biological conclusions and discussion

Recently, the Filippov system has attracted great attention in different fields, since it provides a natural and rational framework for many real-world problems. The threshold policy has been widely used in grazing, harvesting and culling [25,30,31]. In particular, in the scenario of controlling plant disease, the plants are rogued and replanted only when the number of infected plants reaches or exceeds the *ET*. The main purpose of this paper is to use the Filippov system to model this intervention and examine the conditions under which the number of infected plants is eventually maintained below the *ET* while ensuring susceptible plants do not become extinct. Therefore, the Filippov plant disease models developed here describe the disease dynamics associated with cultural strategy and threshold policy. Making use of the qualitative analysis of the global dynamics of the model, we have established conditions under which our objective can be achieved, which are summarized in Table 1.

It is worth noting that the Filippov models described here differ from the state-dependent impulsive differential models discussed by Tang et al. [18] and have many advantages from the point of view of plant disease management and mathematics, although neither system is smooth. First, the trajectories of impulsive models are not continuous, while the trajectories of the Filippov systems proceeding along alternate subsystems are continuous. Secondly, under the state-dependent impulsive modeling approach, the interventions are implemented instantaneously; conversely, in the Filippov systems, when the number of infected plants reaches or exceeds the *ET*, control measures are triggered, the system is

switched into the control system, and interventions last for a duration until to the next switch. Hence, non-instantaneous control is modeled in the Filippov systems. Thirdly, the Filippov systems can give rise to qualitatively new behavior, such as the appearances of various types of equilibria and sliding dynamics. Therefore, it is more meaningful and realistic to use Filippov systems to investigate the development of plant diseases. However, the sliding nature of the Filippov systems makes the study more complicated.

It should be emphasized that, by making full use of the first integral, Lambert W Function and Lyapunov function, we have examined the global dynamics for model (6) with proportional planting rate: the nonexistence of a limit cycle and the existence of a global attractor. The methods used here can be applied to completely analyze many Lotka-Volterra models with first integrals, such as a predation model proposed by Krivan [32]. However, there are limitations for some nonlinear systems without the first integrals. That is because, with the help of analytical solutions or first integrals, we could easily get the trajectories in the phase plane and investigate the global dynamics. The analysis of Section 3 reveals that there does not exist the limit cycle in $G_1 \bigcup G_2$, and the global attractor of Case 3.1, 3.2, 3.3, 3.4, 3.5 refers to $\Gamma^1 \bigcup \Gamma^2$ and its interior, $\omega_1(R_+^2), \omega_2(R_+^2)$, $\omega_1(R_+^2), \omega_2(R_+^2)$, respectively.

The planting and replanting rates are two important factors in determining the dynamical behavior of the system. First, if only p changes among parameters of (6), then our objective can be reached provided the ET is relatively large (i.e. $ET > \frac{\alpha-\eta_1}{\beta}$) and one of the following conditions holds: (i) $0 < p \leqslant \beta ET + \eta_1 - \alpha$; (ii) $p > \beta ET + \eta_1 - \alpha, S_0 \in \Delta$, where $\Delta = (S_{C_{4k+1}}, S_{C_{4k+2}}) \bigcup (S_{C_{4k+4}}, S_{C_{4k+5}})$, $k \geqslant 0$. Secondly, let α change and $\alpha > \eta_1$, $p > \eta_1$ be valid. When the ET is relatively small (i.e. $ET \leqslant p/\beta$), we can achieve the target if we control the parameter α to satisfy $\beta ET + \eta_1 - p < \alpha < \beta ET + \eta_1$, $S_0 \in \Delta$. When the ET is relatively large (i.e. $ET > p/\beta$), we can achieve the target if one of the following conditions holds true: (i) $\alpha \leqslant \beta ET + \eta_1 - p$, (ii) $\beta ET + \eta_1 - p < \alpha < \beta ET + \eta_1, S_0 \in \Delta$. Thirdly, if the ET is fixed, and p and α vary, the goal can be achieved if the parameters satisfy one of the conditions as follows:

(i) $\alpha < \beta ET + \eta_1$, $\alpha + p \leqslant \beta ET + \eta_1$;

(ii) $\alpha < \beta ET + \eta_1$, $\alpha + p > \beta ET + \eta_1, S_0 \in \Delta$.

Consequently, we can use the initial conditions, the planting and replanting rates to design the threshold policy such that the number of infected plants can be maintained below the ET eventually.

It is always postulated that $\upsilon > 0$, $p > 0$ in the Filippov plant disease model (6), which indicates that the replanting and roguing control strategies are implemented simultaneously. What is the result if we only carry out one control? First, assume $\upsilon = 0$, $p > 0$. Here, we take the case that E_1 and E_2 are real equilibria as an example. It follows from Fig. 10 that the trajectory starting from A_1 is closed. These reveal that all trajectories are closed, which gives different dynamic behavior compared with $\upsilon > 0$, $p > 0$. For other cases, we will get similar results. Hence, if we only carry out replanting control when $I > ET$, the goal cannot be achieved. Secondly, suppose $\upsilon > 0$, $p = 0$. The sliding-mode dynamics are described by

$$\frac{dS(t)}{dt} = (\alpha - \beta ET - \eta_1)S(t). \tag{22}$$

There are three situations: 1. E_R^1 and E_V^2; 2. E_V^1 and E_R^2; 3. E_B^1 and E_B^2. The results of the first two situations are the same as those in Cases 3.2 and 3.3, respectively. However, for the third situation, according to (22) and $\frac{\alpha-\eta_1}{\beta} = ET$, we have $dS/dt = 0$ in the sliding region Σ_1, so all points in Σ_1 are pseudoequilibria for (6). Making use of qualitative analysis, it is easy to see that all solutions will eventually stabilize at a point in $\overline{\Sigma_1}$, which is a new phenomenon compared with $\upsilon > 0$, $p > 0$. So we can reach the target in this case. To sum up, if we only implement replanting control, we will fail to achieve our aim. If we only carry out roguing control, our aim may be achieved.

We mention that we here consider the effort to replant or rogue plants to be proportional to the number of plants. This assumption could be initially reasonable from the point of view of mathematics [18]. That is because the proportional roguing cannot lead to negative solutions compared to the relatively large constant roguing. Moreover, the values of the proportional roguing and replanting rates might depend on the availability of workers. Our results indicate that we may not reach our goal mentioned above if the rates are not appropriate. It is interesting to note that the replanting and roguing plants can be modeled by constants, independent of the existing numbers of plants or the number of available workers. We leave this for future work.

The related practical significance for all results obtained in this work can guide us to establish a good treatment program and prevent an intolerable build-up of diseases. Finally, it is essential to link the costs of implementing controls to modeling of plant disease epidemics, to consider other strategies of IDM, such as biological tactics that introduce some natural enemies of the insects who transmit plant diseases in the plant-growth environment. We leave these for further investigations.

Acknowledgements

Research was supported by the National Natural Science Foundation of China (NSFC 11171268), by the Fundamental Research Funds for the Central Universities (08143042), and by the International Development Research Center, Ottawa, Canada (104519-010). R.J.S.? was supported by an NSERC Discovery Grant, an Early Researcher Award and funding from MITACS. For citation purposes, note that the question mark is part of his name.

Appendix A. Methods for analyzing sliding solution

Filippov convex method: The Filippov method associates the following convex combination $M_1(X)$ of the two vectors $F_1(X)$ and $F_2(X)$ to each nonsingular sliding point $X \in \Sigma_1$, i.e.

$$M_1(X) = \lambda F_1(X) + (1-\lambda)F_2(X),$$

where $\lambda = \frac{\langle H_X(X), F_2(X)\rangle}{\langle H_X(X), F_2(X) - F_1(X)\rangle}$. $M_1(X)$ is tangent to Σ_1.

Thus, the sliding-mode dynamics can be determined by

$$\frac{dX(t)}{dt} = M_1(X(t)), \quad X \in \Sigma_1, \tag{A.1}$$

which is smooth on a one-dimensional sliding interval of Σ_1. The solution of (A.1) is the sliding solution.

Utkin equivalent control method: Utkin proposed an equivalent control method to describe the sliding-mode dynamics on the switching line Σ for (2). Assume that a sliding mode exists on Σ, i.e. Σ_1 is non-empty. The Filippov system (2) can be rewritten as

$$\frac{dX(t)}{dt} = M_2(X, \mu_H), \tag{A.2}$$

where the control μ_H is defined as

$$\mu_H = \begin{cases} 0, & \text{if} \quad H(X) < 0, \\ \mu, & \text{if} \quad H(X) > 0, \end{cases} \tag{A.3}$$

with μ a continuous function.

The solution of the equation

$$\frac{dH(t)}{dt} = \frac{\partial H}{\partial X} M_2(X, \mu_H) = 0 \tag{A.4}$$

with respect to μ_H is referred to as "equivalent control". We denote it by μ_H^*. Substituting μ_H with μ_H^* yields

$$\frac{dX(t)}{dt} = M_2(X, \mu_H^*), \quad X \in \Sigma_1, \tag{A.5}$$

which determines the sliding-mode dynamics of the Filippov system (2).

Appendix B. Definitions of Lambert W function and equilibrium

Definition 4.1. [28] The *Lambert W function* is defined to be the multi-valued inverse of the function $z \to ze^z$ satisfying

$$\text{LambertW}(z)\exp(\text{LambertW}(z)) = z.$$

It is easy to see that the function ze^z has the positive derivative $(z+1)\exp(z)$ if $z > -1$. The inverse function of ze^z restricted on the interval $[-1, \infty]$ is defined by LambertW$(0, z)$. For simplicity, LambertW$(0, z) \equiv$ LambertW(z). Similarly, we define the inverse function of ze^z restricted on the interval $(-\infty, -1]$ to be LambertW$(-1, z)$. Now we define the concepts of various types of equilibria for system (2).

Definition 4.2.

(i) A point E is called a *real equilibrium* of (2) if

$$F_1(E) = 0,\ H(E) < 0, \quad \text{or} \quad F_2(E) = 0,\ H(E) > 0.$$

A point E is called a *virtual equilibrium* of (2) if

$$F_1(E) = 0,\ H(E) > 0, \quad \text{or} \quad F_2(E) = 0,\ H(E) < 0.$$

(ii) A point E is called a *pseudoequilibrium* if it is an equilibrium of the sliding mode (A.1) or (A.5), i.e.

$$M_1(E) = 0,\ H(E) = 0, \quad \text{or} \quad M_2(E) = 0,\ H(E) = 0.$$

(iii) A point E is called a *boundary equilibrium* of (2) if

$$F_1(E) = 0,\ H(E) = 0, \quad \text{or} \quad F_2(E) = 0,\ H(E) = 0.$$

It follows from the above definitions that a stable virtual equilibrium is never actually attained since the dynamic change as soon as the trajectory crosses the switching manifold Σ.

Appendix C. Definition of Lyapunov function and theories on the global quality of the Filippov system

Denote the solution from a given initial condition X_0 of (2) by φ_{X_0}, the ω limit set by $\omega(X_0)$ and, for $G \subset R_+^2$,

$$AG(t) \equiv \{X \in R_+^2 | X = \varphi_{X_0}(t) \text{ for some } X_0 \in G\}, \quad \xi(G) \equiv \bigcup_{t \geqslant 0} AG(t).$$

Definition 4.3. [29] A function $V \in C^1(R_+^2)$ is called a *Lyapunov function* of (2) on $G \subset R_+^2$ if it is nonnegative on G and, for all $X \in G$, $\dot{V}^*(X) \equiv \max_{\kappa \in F(X)} \langle \nabla V(X), \kappa \rangle \leqslant 0$,

where $F(X)$ is defined as follows:

$$F(X) \equiv \begin{cases} \{F_1(X)\}, & \text{if} \quad X \in G_1, \\ \{\lambda F_1(S, ET) + (1-\lambda)F_2(S, ET) : \lambda \in [0,1]\}, & \text{if} \quad X \in \Sigma, \\ \{F_2(X)\}, & \text{if} \quad X \in G_2. \end{cases} \tag{C.1}$$

Proposition 4.1. [29] (LaSalle's Invariance Principle) *Suppose that $G \subset R_+^2$ is an open set which satisfies $\omega(G) \equiv \bigcup_{x \in G} \omega(X) \subset \xi(G)$. Let every Filippov solution φ_{X_0}, $X_0 \in G$, of (2) be unique and defined for all $t \geqslant 0$, and $V : R_+^2 \to R$ be a Lyapunov function of (2) on $\xi(G)$. Then $\omega(G)$ is a subset of the largest positively invariant subset of $\overline{\Lambda}$, where $\Lambda \equiv \{X \in \overline{G} | \dot{V}^*(X) = 0\}$.*

Corollary 4.1. [29] *Assume that G and $V : R_+^2 \to R$ satisfy Proposition C.1 and $R_+^2 \setminus G$ is repelling, in the sense that all solutions stay in $R_+^2 \setminus G$ for only a finite time. Let $\omega(R_+^2) = \omega(G)$ be bounded. Then $\overline{\omega(R_+^2)}$ is globally asymptotically stable.*

Appendix D. The proof of Theorem 3.1

Proof. If $k = 1$, according to (12) it is easy to illustrate that (14) holds. Assume that (14) holds true for $k = N$, i.e.

$$\begin{aligned} &S_{C_{4N+2}} = \Phi_3^{N-1}\Phi_1(\widetilde{S}_2), \quad S_{C_{4N+3}} = \Phi_3^{N-1}\Phi_1\left(\frac{\eta_2 + \upsilon}{\beta}\right), \\ &S_{C_{4N+4}} = \Phi_3^{N-1}\Phi_2(\widetilde{S}_2), \quad S_{C_{4N+5}} = \Phi_3^{N-1}\Phi_2\left(\frac{\eta_2}{\beta}\right). \end{aligned} \tag{D.1}$$

If $k = N + 1$, then the paths of the corresponding critical trajectories can be shown as follows:

(I) $\Upsilon_{N+1,N+1}^{4N+5} : C_{4N+6} \to D_{4N+6} \to E_{4N+1} \to C_{4N+2}$;
(II) $\Upsilon_{N+1,N+1}^{4N+6} : C_{4N+7} \to D_{4N+7} \to E_{4N+2} \to C_{4N+3}$;
(III) $\Upsilon_{N+1,N+2}^{4N+7} : C_{4N+8} \to D_{4N+8} \to E_{4N+3} \to C_{4N+4}$;
(IV) $\Upsilon_{N+1,N+2}^{4N+8} : C_{4N+9} \to D_{4N+9} \to E_{4N+4} \to C_{4N+5}$,

where $C_{4N+2}, C_{4N+3}, C_{4N+4}, C_{4N+5}$ are the initial points of the critical trajectories $\Upsilon_{N,N}^{4N+1}$, $\Upsilon_{N,N}^{4N+2}$, $\Upsilon_{N,N+1}^{4N+3}$ and $\Upsilon_{N,N+1}^{4N+4}$, respectively. Due to the results (D.1) and the facts that

$$S_{E_{4N+1}} = \Psi_1(S_{C_{4N+2}}), \quad S_{D_{4N+6}} = \Psi_2(S_{E_{4N+1}}), \quad S_{C_{4N+6}} = \Psi_3(S_{D_{4N+6}}),$$

we have

$$\begin{aligned} S_{C_{4N+6}} &= \Psi_3 \circ \Psi_2 \circ \Psi_1(S_{C_{4N+2}}) = \Phi_3(S_{C_{4N+2}}) = \Phi_3 \circ \Phi_3^{N-1}\Phi_1(\widetilde{S}_2) \\ &= \Phi_3^N\Phi_1(\widetilde{S}_2). \end{aligned}$$

Using the same method, we get the following conclusions

$$\begin{aligned} &S_{C_{4N+7}} = \Phi_3^N\Phi_1\left(\frac{\eta_2 + \upsilon}{\beta}\right), \quad S_{C_{4N+8}} = \Phi_3^N\Phi_2(\widetilde{S}_2), \\ &S_{C_{4N+9}} = \Phi_3^N\Phi_2\left(\frac{\eta_2}{\beta}\right). \end{aligned}$$

Therefore, the conclusion (14) is true for $k = N + 1$, which demonstrates that (14) holds true for all positive integers k. □

References

[1] R.W. Gibson, J.P. Legg, G.W. Otim-Nape, Unusually severe symptoms are a characteristic of the current epidemic of mosaic virus disease of cassava in Uganda, Ann. Appl. Biol. 128 (1996) 479.
[2] T. Iljon, J. Stirling, R.J. Smith?, A mathematical model describing an outbreak of Fire Blight, in: S. Mushayabasa, C.P. Bhunu (Eds.), Understanding the Dynamics of Emerging and Re-emerging Infectious Diseases Using Mathematical Models, 2012, pp 91–104.
[3] L.M.C. Medina, I.T. Pacheco, R.G.G. Gonzalez, et al., Mathematical modeling tendencies in plant pathology, Afr. J. Biotechnol. 8 (2009) 7399.
[4] R.A.C. Jones, Determining threshold levels for seed-borne virus infection in seed stocks, Virus Res. 71 (2000) 171.
[5] R.A.C. Jones, Using epidemiological information to develop effective integrated virus disease management strategies, Virus Res. 100 (2004) 5.
[6] T.T. Zhao, S.Y. Tang, Plant disease control with economic threshold, J. Biomater. 24 (2009) 385.
[7] H.R. Thieme, J.A.P. Heesterbeek, How to estimate the efficacy of periodic control of an infectious plant disease, Math. Biosci. 93 (1989) 15.
[8] F. van den Bosch, N. McRoberts, F. van den Berg, L.V. Madden, The basic reproduction number of plant pathogens: matrix approaches to complex dynamics, Phytopathology 98 (2008) 239.

[9] F. van den Bosch, M.J. Jeger, C.A. Gilligan, Disease control and its selection for damaging plant virus strains in vegetatively propagated staple food crops; a theoretical assessment, Proc. R. Soc. B 274 (2007) 11.
[10] F. van den Bosch, A.M. Roos, The dynamics of infectious diseases in orchards with roguing and replanting as control strategy, J. Math. Biol. 35 (1996) 129.
[11] M.S. Chan, M.J. Jeger, An analytical model of plant virus disease dynamics with roguing, J. Appl. Ecol. 31 (1994) 413.
[12] J.C. Zadoks, R.D. Schein, Epidemiology and Plant Disease Management, Oxford University, New York, 1979.
[13] L.V. Madden, G. Hughes, F. van den Bosch, The Study of Plant Disease Epidemics, The American Phytopathological Society, St. Paul, Minnesota, USA, 2007.
[14] S. Fishman, R. Marcus, H. Talpaz, et al., Epidemiological and economic models for the spread and control of citrus tristeza virus disease, Phytoparasitica 11 (1983) 39.
[15] V. Capasso, Mathematical Structures of Epidemic Systems, Springer-Verlag, Berlin, 1993.
[16] S.Y. Tang, Y.N. Xiao, R.A. Cheke, Multiple attractors of host-parasitoid models with integrated pest management strategies: eradication, persistence and outbreak, Theor. Popul. Biol. 73 (2008) 181.
[17] S.Y. Tang, R.A. Cheke, Models for integrated pest control and their biological implications, Math. Biosci. 215 (2008) 115.
[18] S.Y. Tang, Y.N. Xiao, R.A. Cheke, Dynamical analysis of plant disease models with cultural control strategies and economic thresholds, Math. Comput. Simul. 80 (2010) 894.
[19] A.F. Filippov, Differential Equations with Discontinuous Righthand Sides, Kluwer Academic, Dordrecht, 1988.
[20] V.I. Utkin, Sliding Modes in Control and Optimization, Springer, Berlin, 1992.
[21] V.I. Utkin, J. Guldner, J.X. Shi, Sliding Mode Control in Electro-mechanical Systems, second ed., Taylor & Francis Group, 2009.
[22] M.D. Bernardo, C.J. Budd, A.R. Champneys, et al., Bifurcations in nonsmooth dynamical system, SIAM Rev. 50 (2008) 629.
[23] B. Brogliato, Nonsmooth Mechanics, Springer-Verlag, NY, 1999.
[24] M.I.S. Costa, Harvesting induced fluctuations: insights from a threshold management policy, Math. Biosci. 205 (2007) 77.
[25] M.I.S. Costa, E. Kaszkurewicz, A. Bhaya, L. Hsu, Achieving global convergence to an equilibrium population in predator–prey systems by the use of a discontinuous harvesting policy, Ecol. Model. 128 (2000) 88.
[26] F. Dercole, A. Gragnani, S. Rinaldi, Bifurcation analysis of piecewise smooth ecological models, Theor. Popul. Biol. 72 (2007) 197.
[27] M. di Bernardo, P. Kowalczyk, A. Nordmark, Bifurcation of dynamical systems with silding: derivation of normal-form mappings, Physica D 170 (2002) 175.
[28] R.M. Corless, G.H. Gonnet, D.E.G. Hare, et al., On the Lambert W function, Adv. Comput. Math. 5 (1996) 329.
[29] D.S. Boukal, V. Krivan, Lyapunov functions for Lotka–Volterra predator-prey models with optimal forging behavior, J. Math. Biol. 39 (1999) 493.
[30] M.I.S. Costa, L.D.B. Faria, Integrated pest management: theoretical insights from a threshold policy, Neotrop. Entomol. 39 (2010) 1.
[31] M.E.M. Meza, A. Bhaya, E. Kaszkurewicz, M.I.da S. Costa, Threshold policies control for predator–prey systems using a control Liapunov function approach, Theor. Popul. Biol. 67 (2005) 273–284.
[32] V. Krivan, Effects of optimal antipredator behavior of prey on predator–prey dynamics: the role of refuges, Theor. Popul. Biol. 53 (1998) 131.